Cyclist conflict behavior in shared spaces

by

Anna Marbus

TUDelft

Cyclist conflict behavior in shared spaces

by

Anna Marbus

to obtain the degree of Master of Science
at the Delft University of Technology,
to be defended publicly on April 17, 2025 at 9 AM.

Student number: 4437381
Project Duration: June, 2024 - April, 2025
Supervisors: Prof. Dr. Ir. R. Happee
                   Dr. J. K. Moore
                   Ir. C. Konrad

An electronic version of this thesis is available at http://repository.tudelft.nl/.

TUDelft

Preface

Two years ago, in the preface of my Master's thesis in Biomedical Engineering, I wrote that if everything went well, I would get to write another one someday. Well, here we are! I guess things did go right, because I am sitting here, once again, writing the preface of my thesis. Never in a million years would I have expected that when I started Clinical Technology, literally ten years ago, I would end up graduating with a Master's focusing on programming and robot dynamics. Back in 2015, when I started Clinical Technology, my friends and I were incredibly lucky to have Eris, the one person in our group who actually understood programming. She was the one who patiently explained everything to the rest of us when we had no clue what we were doing. Ironically, the joke is on me now, because somehow, I became Eris. I am now one of those geeks who actually knows their way around Python, MATLAB, and C++. Even though my interests have shifted over time, a lot has stayed the same. My friends, who are still sometimes shocked that I actually have a functional brain and not just the appearance of a hairdresser, have always been by my side. They have been my personal cheerleaders, keeping me sane during exams and deadlines.

Besides my friends in Lisse, Leiden, and Delft, I have the most amazing parents. My mom, my moral support, who wrote excuse notes so I could skip PE, and my father, whom she fondly called "een ijsbeer" whenever he raised his voice over a mathematical equation at the kitchen table, insisting: "Anna, dit is de basis!". But, if it were not for my dad, I would not be where I am today. He literally got me through high school, especially since I was not exactly the best-behaved student. The truth is, I am naturally lazy. Why ride a bike when you can just drive? And why fix your own tire pressure when you can just call the ANWB? My parents already know how grateful I am for all their support, but once again: thank you. From the bottom of my heart. I do not know what I would do without your love, your humor, and your endless support.

This brings me to the bike lab crew at the university. Let's be real, when it comes to practical things like welding, 3D printing, or even sawing a broom, I am completely hopeless. A year ago, I had never even touched an Arduino. Despite my proclaimed status as a "grote tuttebel" with limited hands-on skills, you were always there to help me. Whether it was fixing things or just opening the door for me because I forgot my card again. So, a huge thank you to Bram, Marcel, Timon, and Eelco for all the help and for the countless laughs we had over the dumbest things. I should probably apologize for constantly distracting you. But hey, from now on, you can finally work in peace and maybe, just maybe, finish your literature studies.

Then, my supervisors. Riender, once again, my main supervisor, I am truly glad you were not completely fed up with me yet. Through you, I met Christoph and Jason. Christoph, your support throughout this project was incredible. During our meetings, you showed me how much you truly cared about my work. You are such a great person, and any future Master's student would be lucky to have you as a daily supervisor. And then, Jason, Professor Bicycle, thank you for your guidance throughout this project. I will miss my role as MC, and, sorry for ever thinking you were 45 years old. I was joking. Finally, special thanks to Jules, Gabriele, Joost, Benjamin, and my golden coffee guy for always ensuring my little fish and I had enough caffeine to survive our days. Of course, we appreciated you for more than just the coffee.

Abstract

Infrastructure deficiencies and problematic interactions with other road users are identified as factors that increase the risk of cyclist crashes. This underscores the need for developing more adequate cycling infrastructure and environments to mitigate such crashes. Microscopic simulation models provide a valuable tool for assessing the potential impact of infrastructure modifications before real-world implementation. However, realizing this potential requires thorough investigation of cyclist behavior to inform model development, calibration, and validation. This study contributes experimental data designed to enhance the accuracy and facilitate the validation of these models.

A controlled field experiment was conducted to examine cyclist interaction behaviors across four distinct scenarios characterized by varying encounter angles between cyclists. These scenarios were designed to replicate unstructured, real-world interactions occurring in open-space environments, thereby simulating interactions in the absence of formal traffic rules.

The participants, paired in dyads, rode instrumented bicycles, enabling the collection of kinematic data for subsequent analysis of cyclists' path and speed adjustments during close-proximity interactions. The analysis indicated that cyclists predominantly adjusted their trajectories rather than their velocities in response to these interactions. These adjustments, collectively referred to as avoidance strategies, exhibited variation across different encounter scenarios, suggesting that cyclists modify their avoidance behaviors based on both the behavior of the interacting cyclist and the specific encounter angle.

These avoidance strategies form the foundation of yielding behavior among cyclists. To identify the factors influencing this behavior, a statistical model was developed incorporating predictors such as difference in time-to-arrival (DTA), initial velocity difference, gender, and the cessation of pedaling. The model revealed that cyclists who arrived first at the boundary of a predefined interaction area, exhibited higher velocities, and approached from the left were more likely to yield relative to their interaction partner. The model demonstrated a predictive accuracy of 80%.

While this study establishes a foundational framework for the enhancement and validation of traffic simulation models, the relatively small dataset represents a limitation. Although data augmentation techniques could be utilized to deepen the understanding of the determinants of avoidance strategy selection, the acquisition of additional real-world observational data is recommended. Expanding the dataset would not only refine microscopic traffic simulations but also improve the statistical model, potentially facilitating its integration into automated vehicle (AV) systems. Given the current limitations of AVs in predicting cyclist behavior, further improvements in the model's predictive accuracy are imperative for successful AV integration.

Contents

Nomenclature

AIC	Akaike Information Criterion
AV	Automated Vehicle
BIC	Bayesian Information Criterion
DTA	Difference in Time Arrival
GNSS	Global Navigation Satellite System
ICC	Intraclass Correlation Coefficient
IMU	Inertial Measurement Unit
LRT	Likelihood Ratio Test
PA	Path Adjustment
RTK	Real Time Kinematics
TTC	Time-To-Collision
UTC	Coordinated Universal Time
VIF	Variance Inflation Factor
VS	Velocity Selection

List of Figures

List of Tables

Introduction

1.1. Background and significance

As cycling's popularity grows, its presence in cities becomes increasingly common. It is a key component of sustainable urban mobility for the environment and public health, and an alternative to driving cars (Nikitas et al., 2021). Notably, the Netherlands leads Europe with 27% of trips made by bicycle (Buehler, 2018). Unfortunately, the rising popularity of cycling is accompanied by an increase in bicycle-related road crashes. Due to cyclists' vulnerability to serious injuries, riding a bike is estimated to be seven times more unsafe than traveling by car, posing a serious concern for public health agencies and practitioners (Feleke et al., 2017).

Studies identified the influence of infrastructure and problematic interactions with other users as factors that increase the risk of cyclist crashes (Kim et al., 2012; S. Useche et al., 2018a; S. A. Useche et al., 2018b). This highlights the need for developing more adequate cycling infrastructure and environments to reduce cyclist crashes. Microscopic simulation models offer a powerful tool to evaluate the potential impact of infrastructure changes and cycling policies on both traffic flow and safety before real-world implementation (Dias et al., 2023). However, their ability to accurately represent real-world scenarios hinges on a deep understanding of cyclist interactions with other road users. This deep understanding involves more than just recognizing observable behaviors; it requires analyzing the underlying motivations and decision-making processes that lead to specific behaviors. To achieve this level of insight, comprehensive research into cyclist behavior is necessary, which can then inform model development, calibration, and validation.

Beyond evaluating the impact of infrastructure changes, these models play a vital role in the safe integration of automated vehicles (AVs). This is particularly important because cyclist behavior, especially in conflict scenarios, is highly heterogeneous due to the influence of numerous factors. As described by Chin and Quek (1997), traffic conflict scenarios involve observable situations where two or more road users approach each other in space and time, creating a risk of collision if their movements remain unchanged. Given the limitations of AV technology in understanding complex human behaviors like cyclist actions, traffic simulation models can predict potential AV responses to various cyclist maneuvers. This predictive capability helps identify potential collision scenarios and areas for improvement in AV perception and decision-making algorithms. However, the validity of these models relies heavily on robust validation against real-world data. By comparing simulated cyclist behavior with observed behavior from field experiments, researchers can identify and address discrepancies, ensuring the model's accuracy and reliability.

The objective of this study is to contribute experimental data that can enhance the accuracy of simulation models and support the validation process. To achieve this, a controlled field experiment was designed to study the behavior of cyclists during close encounters in open-space scenarios. The study focused on four distinct interaction scenarios characterized by varying the angle of encounter between two cyclists. These scenarios were designed to replicate unstructured, real-world interactions in the ab-

sence of defined traffic rules. Instrumented bicycles were utilized to acquire comprehensive kinematic data, encompassing both positional and rotational kinematics. This dataset served as the basis for analyzing cyclist behavior during conflict scenarios. Furthermore, this study aims to identify the factors influencing cyclists' path and speed adjustments that result in yielding behavior. These findings offer valuable insights for validating simulation models designed to enhance cyclist safety in infrastructure design and the development of autonomous systems.

1.2. Research questions

This study comprises two parts. The first part investigates the kinematics of interacting cyclists, focusing on analyzing their trajectories and velocity profiles. This directly addresses the first research question:

> *How do cyclists adjust their path and speed to avoid collisions in close inter-   (1)
> actions, and how do these strategies vary across different scenarios?*

The second part of this study examines the factors influencing path and speed adjustments, with a focus on yielding behavior, to address the following research question:

> *What interaction characteristics underlie path and speed adjustments involv-   (2)
> ing yielding behavior?*

In this context, yielding is defined as the behavior of a cyclist who, in a close interaction with another cyclist, crosses the intersection last as a result of a priority resolution process.

1.3. Thesis outline

This thesis comprises nine chapters, each contributing to a comprehensive investigation of cyclist behavior in interaction scenarios. Chapter 2 describes the experimental methodology, including the study protocol and data acquisition procedures. Chapter 3 outlines the data processing methods, detailing the pre-processing steps necessary for the subsequent analyses. Chapter 4 presents the kinematic analysis methodology, which addresses the first research question by examining path and speed adjustments. Chapter 5 introduces the statistical modeling framework used to explore interaction characteristics underlying yielding behavior, thereby addressing the second research question. Chapter 6 reports the results of the kinematic analysis, while Chapter 7 focuses on the outcomes of the statistical modeling. Chapter 8 critically evaluates the study's limitations and proposes directions for future research. Finally, Chapter 9 synthesizes the key findings, integrating insights from both the kinematic and statistical analyses to provide a comprehensive response to the two research questions.

2

Experimental Setup

This chapter provides a detailed description of the experimental setup employed in this study. It begins with an overview of the study participants, outlining their relevant characteristics. Subsequently, the experimental protocol is described, detailing the procedures followed throughout the study. Finally, the chapter presents the data collection methods, including a technical description of the instrumentation and equipment integrated into the bicycles used in the study.

2.1. Participants

Twenty participants (10 males, 10 females) were recruited from Delft University of Technology to participate in a cycling experiment investigating cyclist interaction behavior. The experiment was conducted on an experimental track located behind the Faculty of Mechanical Engineering (Mekelweg 2, Delft, Netherlands). Participants, aged 22 to 42 (mean = 25.9, SD = 2.2), interacted with another cyclist in a semi-circular arrangement resembling an open-space environment. All participants were experienced bicycle riders. Participants were paired to form male-female dyads, a strategy employed to address potential biases associated with single-gender studies and to investigate possible gender-based differences (Holdcroft, 2006). Participants reported an average of 5.5 hours of cycling per week (SD = 3.3). Their primary motivations for cycling were commuting (n = 16), recreation (n = 3), sport (n = 4), and touring (n = 4).

2.2. Experimental protocol

In each trial, participants, paired in male-female dyads, rode bicycles, commencing from one of eight predefined starting positions. These starting positions, designated A through H, are illustrated in Figure 2.1. These positions were clearly marked on the experimental track using cardboards to ensure consistency and visibility. In each trial, one participant started on the left side of the semi-circle (positions A through D) and traveled toward a destination on the right. Simultaneously, the other participant started from a position on the right side (positions E through H) and proceeded toward a destination on the left side of the semi-circle.

Throughout this study, scenarios in which participants initiated their trial from the left side of the semi-circle are designated as 45^D, 90^C, 135^B, and 180^A. The numerical value represents the encounter angle, and the alphabetical character denotes the starting position. Similarly, scenarios initiated from the right side of the semi-circle are designated as 45^E, 90^F, 135^G, and 180^H. As part of the experimental protocol, participants cycled on heavy e-bikes with the electric propulsion assistance turned off and the transmission fixed in gear 3. Prior to the experiment, participants were afforded time to familiarize themselves with the bicycle's dynamics and control characteristics to ensure confident and consistent handling throughout the trials.
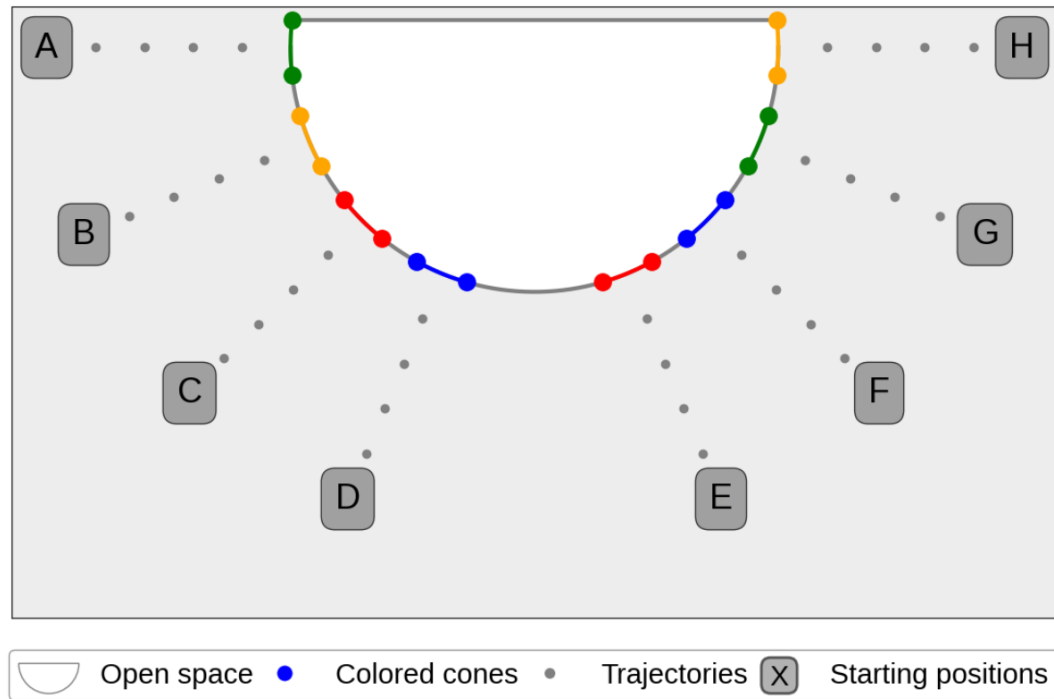
Figure 2.1: Schematic representation of the experimental setup. *Colored dots* indicate the positions of cones on the ground, forming passing ports. Letters denote participant starting positions, which were marked on the track with corresponding cardboard markers. The *grey dotted line* represents the trajectory toward the semi-circular interaction area, where colored cones defined the passing ports. This semi-circular area constituted the open space within which participants' paths intersected as they proceeded to their respective destinations.

Upon receiving the start signal, a loud clap produced by striking two wooden sticks together, participants traversed a 10-meter path from their respective starting positions toward a pair of colored cones. The trajectory of this path is indicated by the grey dots in Figure 2.1. Participants were instructed to maintain a constant velocity of 10 km/h during this traversal, which was monitored in real-time via their bicycle-mounted speed displays. This speed regulation ensured synchronized entry into the semi-circular arrangement, facilitating authentic interactions between cyclists.

After participants traversed designated passing ports, marked by pairs of identically colored cones and indicated by the colored dots in Figure 2.1, they entered a semi-circular arrangement with a 9-meter radius. Within this shared space, participants navigated freely, adjusting their speed and trajectory as necessary. Each participant interacted with another cyclist who was also proceeding to their respective destination. Importantly, participants were not informed of each other's intended destination, ensuring that interactions unfolded naturally. This setup required active coordination, as participants were instructed to navigate the space as they would in a real-world open environment, while remaining attentive to avoid collisions. It is important to note that communication between participants was strictly prohibited during the experiment. This restriction applied to both auditory communication (e.g., talking, bell ringing) and non-verbal communication (e.g., hand gestures).

The experiment featured four distinct encounter scenarios with angles of 45°, 90°, 135°, and 180°, as schematically illustrated in Figure 2.2. Each participant experienced all four scenarios from both sides of the semi-circle, yielding eight trials. To minimize learning effects, trials were conducted in a predetermined, counterbalanced order, with each trial performed only once. This design yielded a sufficient dataset while mitigating potential participant fatigue.
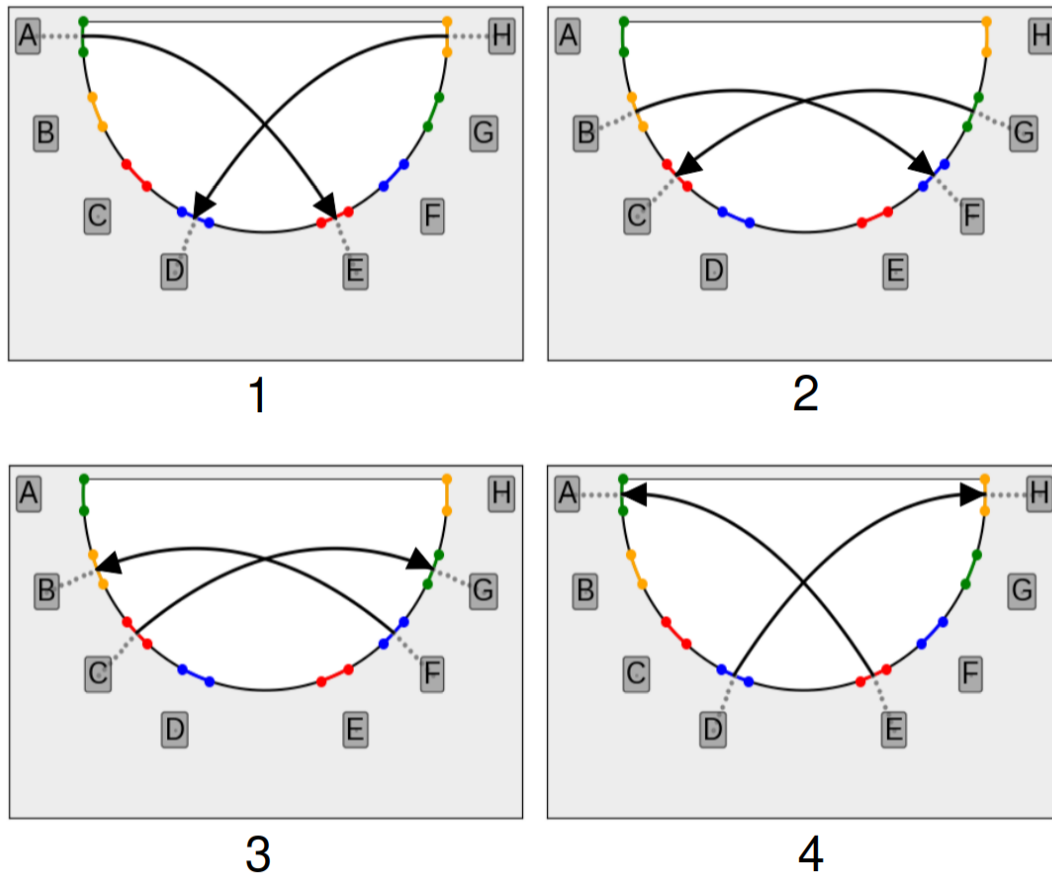
Figure 2.2: Schematic representation illustrates the four encounter scenarios. *Grey dotted lines* connecting letters to the semi-circle depict the intended trajectories, where participants aim to maintain a velocity of 10 km/h The *black arrows* indicate the direction of each participant. Subplot 1 showcases the 180° encounter scenario, subplot 2 the 135° encounter scenario, and subplots 3 and 4 the 90° and 45° encounter scenarios, respectively. Each participant completes eight trials, alternating between starting on the left and right sides of the semi-circle.

The angles for each encounter scenario, shown in Figure 2.2, define the relative starting positions of the participants. These angles were deliberately chosen to ensure that cyclists crossed paths within the semi-circle, promoting active interaction. The experimental track's dimensions and uneven surface characteristics, comprising two distinct tile types and a longitudinal depression, were carefully considered. To minimize surface variability during cyclist interactions, encounters were conducted exclusively on a section of the track comprised of a single tile type, ensuring a uniform surface and preventing potential confounding effects. A consistent turning angle of 110°, representing the angle between the participant's starting position and destination, was implemented across all scenarios to minimize variability and account for its potential influence on experimental outcomes.

As illustrated in Figure 2.2, participants' destinations did not coincide with the starting position of the other participant. This strategic assignment was implemented to enhance the safety of the participants.

Figure 2.3 presents two photographs captured during the experiment, illustrating the placement of the cones previously depicted schematically in Figures 2.1 and 2.2. Additionally, the images highlight the uneven surface of the track, particularly in the 45° scenario, where participants encountered the longitudinal depression in the surface as they entered the semi-circle.
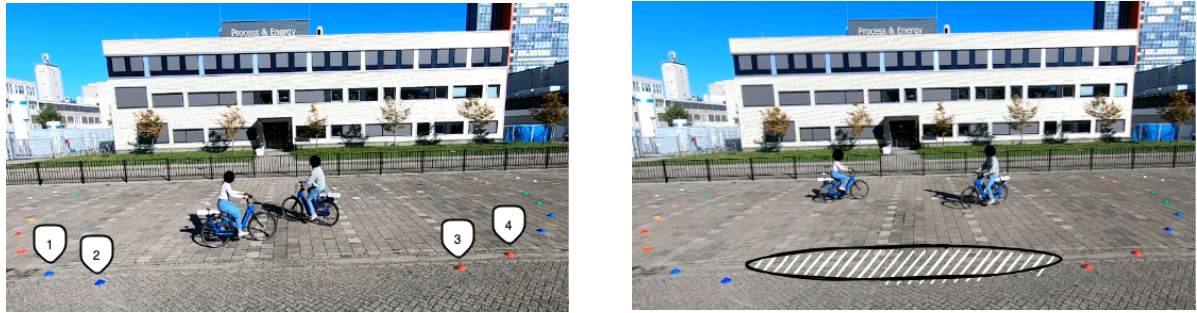
Figure 2.3: Photographs of participants conducting the experiment. The images show two participants navigating the experimental setup on instrumented bicycles. The left image illustrates the 45° encounter scenario, where cones labeled 1 and 2 indicate the starting position of the first cyclist, and cones labeled 3 and 4 indicate the starting position of the second cyclist. The right image depicts the 135° encounter scenario, with the oval-striped area highlighting an uneven surface containing a noticeable depression.

During the experiment, participants received instructions about their starting positions and destinations from an information sheet attached to the rear rack of their bicycles, as presented in Tables 2.1 and 2.2. This ensured that participants had visual access to the necessary information prior to each trial, removing the need for verbal instructions from the experimenter. By providing written rather than verbal instructions, potential split-attention effects were minimized, aligning with cognitive load theory, which emphasizes the limited capacity of working memory (Jong, 2009). Each interacting pair was randomly assigned bicycles equipped with one of two distinct information sheets.

Table 2.1: Information sheet attached to the rear rack of the first bicycle, with starting positions designated by letters and destinations indicated by cone colors on the track.

Trial	Starting position	Destination
T1	B	Blue
T2	G	Red
T3	A	Red
T4	E	Green
T5	D	Orange
T6	F	Orange
T7	C	Green
T8	H	Blue

Table 2.2: Information sheet attached to the rear rack of the second bicycle, with starting positions designated by letters and destinations indicated by cone colors on the track.

Trial	Starting position	Destination
T1	G	Red
T2	B	Blue
T3	H	Blue
T4	D	Orange
T5	E	Green
T6	C	Green
T7	F	Orange
T8	A	Red

Tables 2.1 and 2.2 show that starting positions were labeled with letters, corresponding to the cardboards placed on the track, while destinations were indicated by the color of the cone pairs through which participants had to cycle. This approach was implemented to prevent confusion and ensure clarity in navigation. Furthermore, no participants reported difficulties in interpreting the visual instructions due to potential color vision deficiencies.

Following each trial, participants completed a questionnaire assessing their perceived safety during the interaction and the ease with which they reached their destination. The questionnaire, provided in Appendix A, was affixed to the bicycle's rear rack, along with a pencil. After each trial, participants dismounted and completed the questionnaire before commencing the subsequent trial.

Upon completing all eight trials and filling out the questionnaire after each trial, participants were instructed to cycle the experimental track without any interaction with another cyclist. This required them to repeat the eight trials under identical conditions, but in the absence of another cyclist. These trajectories, referred to as reference trajectories, serve as baseline measurements, representing cyclists' natural trajectories and velocity profiles in the absence of external interactions. Each participant completed these reference trajectories twice to ensure consistency and reliability in the baseline data.

2.3. Data collection

This study employed two independent data acquisition systems, mounted on the rear racks of Gazelle Chamonix HMS bicycles, to collect kinematic data. Additionally, self-reported data was obtained through structured questionnaires, enabling the assessment of participants' subjective experiences.

2.3.1. Kinematic data collection

Position and velocity data were captured using the Piksi Multi Evaluation Kit (Swift Navigation, San Francisco, USA). Hereafter, this system is referred to as the Piksi Multi system. This system utilizes Global Navigation Satellite System (GNSS) technology for high-precision positioning and incorporates an onboard MEMS inertial measurement unit (IMU) for additional motion sensing. The Piksi Multi system consists of an evaluation board connected to a GNSS antenna and is powered by an external power supply. To minimize potential GNSS signal disruptions, the GNSS antenna was mounted on a 10 cm wooden pole. Raw GNSS data, sampled at 10 Hz, and IMU data, sampled at 100 Hz, were recorded to a micro SD card. To enhance the accuracy of raw GNSS data for subsequent analysis, real-time kinematics (RTK) was employed. RTK, a high-precision GNSS technique, leverages correction data from a reference base station. The details of this processing procedure are presented in Chapter 3.

The second data acquisition system, referred to as the cadence system, comprised a magnetic reed switch to detect cyclists' pedaling activity and a MPU-9250 Breakout IMU (SparkFun, Niwot, USA). For the cadence system, a magnet was affixed to the pedal, and a corresponding reed switch was mounted on the bicycle frame. Both the reed switch and IMU were interfaced with a Teensy 4.1 microcontroller (PJRC, Sherwood, USA). Data were sampled at 100 Hz. This microcontroller unit, powered by an external supply, was securely mounted on the bicycle's rear rack.

Figure 2.4 illustrates the experimental bicycle setup for data acquisition, featuring the custom-designed housing for the Piksi Multi system and the cadence system. To ensure consistency in data collection, both bicycles used in the experiment, along with the measurement systems mounted on their rear racks, were identical. The left image highlights the housing for the Piksi Multi system and the cadence system. Instructions, outlined in Tables 2.1 and 2.2, are affixed to the top along with the questionnaire, which will be discussed in the following subsection. The right image provides a clearer interpretation of the setup by incorporating numerical labels for the various components of the data acquisition system.

Figure 2.4: Experimental bicycle setup used for data acquisition. The left image shows the data collection systems housed and mounted on the bicycle's rear rack. The right image provides a more detailed view of the data acquisition systems. The numbered labels indicate the individual components: 1) Teensy 4.1 microcontroller, 2) SparkFun MPU-9250 Breakout IMU, 3) evaluation board, 4) GNSS antenna, and 5) external power supply. The left subfigure illustrates the housing of the data acquisition systems and their attachment to the rear rack of the bicycle. Notably, the GNSS antenna is mounted on a wooden to minimize potential GNSS signal disruptions.

2.3.2. Self-reported data collection

As previously mentioned, in addition to kinematic data collection, this study also gathered participant-specific information through a series of questionnaires. Participants completed a pre-experiment questionnaire assessing demographics and cycling experience, followed by a post-experiment questionnaire evaluating their overall experience with the study. As detailed in Section 2.2, after each trial, participants completed a short questionnaire, rating the perceived safety and intuitiveness of the interaction. This questionnaire consisted of closed-ended questions, with responses recorded on a five-point scale. It is important to note that a score of 5 represented a high level of comfort and the perception of an easy interaction, whereas a score of 1 indicates the lowest level of comfort and the perception of a difficult interaction. All questionnaires are provided in Appendix A.

3

Data Processing

Following data collection, appropriate data processing is required. This chapter begins with the data preparation phase, detailing the procedures used to process and refine the raw data obtained from the measurement systems, ensuring its suitability for subsequent analysis in Python. This is followed by a detailed description of the time synchronization process, which aligns the data from the two independent data acquisition systems to a common timeframe, ensuring temporal consistency.

3.1. Data pre-processing

As described in Section 2.3, the Piksi Multi system acquired both position and velocity data. Due to the distinct characteristics of these data types, separate pre-processing methodologies were employed. The subsequent subsections detail the pre-processing procedures applied to the position data, followed by those applied to the velocity data.

3.1.1. Position data

The Piksi Multi system records raw GNSS data in .sbp (Swift Binary Protocol) format, a communication protocol for Swift Navigation devices. However, despite the meter-level accuracy of this data, centimeter-level accuracy is required for high-resolution analysis of cyclist interaction behavior. This is achieved through RTK, which enhance positional accuracy by compensating for GNSS signal errors. The correction process compares signals received at a precisely known reference station with those recorded by the Piksi Multi system. The discrepancies between these signals are then used to adjust the position data, reducing measurement errors (Li et al., 2022). In this study, the TU Delft GNSS Fieldlab, within the Faculty of Electrical Engineering, Mathematics, and Computer Science, served as the reference station. The high-rate RINEX data from the reference station were downloaded from the TU Delft GNSS website.

RTK processing was performed using RTKLIB 2.4.3 (Takasu, Tokyo, Japan). RTKLIB generated corrected position data, containing geographic coordinates and epoch timestamps, in .pos (Position) format. These files were then imported into Python 3.8 (Python Software Foundation, Beaverton, USA). The position data was segmented to retain only trajectory segments within the defined semi-circular region of interest.

To precisely define the boundary of the semi-circle, an experimental procedure was conducted. A measuring tape was anchored at the center of the semi-circle, and the Piksi Multi system was systematically moved along the arc four times, recording GNSS coordinates at each pass. These recorded positions were then processed using the same differential correction methodology described earlier. To establish a representative boundary, the corrected coordinates were averaged, resulting in a single set of geographic coordinates defining the semi-circle's edge.

3.1.2. Velocity data

In contrast to position data, velocity data did not necessitate differential corrections. Horizontal velocity data and corresponding timestamps were recorded in .csv (Comma-Seperated Values) format, facilitating direct import into Python without format conversion. However, time synchronization was required to align velocity and position data.

Velocity timestamps are recorded in Coordinated Universal Time (UTC), whereas position data are recorded in GPS time, which is 18 seconds ahead of UTC (Kumar et al., 2021). To synchronize both datasets, 18 seconds were added to each UTC timestamp in the velocity data file, aligning it with the GPS time used for position data. This adjustment ensures that both datasets correspond to the same point in time, expressed in GPS time. Finally, in accordance with the position data processing protocol, the velocity data was segmented to isolate the trajectory segments located within the defined semi-circular area region of interest.

3.2. Time synchronization

In addition to synchronizing positional and velocity data, it is essential to ensure time synchronization between the two independent measurement systems, the Piksi Multi system and the cadence system. This synchronization is crucial for accurately integrating data collected from both systems, which were mounted on each of the bicycles. To achieve this, a unified timeframe must be established across all systems and bicycles, ensuring temporal alignment for consistent and reliable data analysis.

The cadence system operates on a relative timescale, where data logging begins at an arbitrary reference point. In contrast, the Piksi Multi system utilizes high-precision GPS time, with a resolution of 0.00001 ms (Swift Navigation, 2024). This high accuracy is derived from a network of synchronized atomic clocks onboard GPS satellites (Ramsey, 1983). Since both the Piksi Multi system and the cadence system incorporate an IMU, the x-axis gyroscope data, corresponding to the bicycle's roll axis, is used as the basis for time synchronization. This choice is due to the distinct peaks generated during a pre-calibration maneuver, in which a brief, controlled shaking motion is applied to the bicycle while both systems are mounted on the rear rack. The induced motion generates identifiable sinusoidal peaks in the x-axis gyroscope data from each IMU, facilitating subsequent synchronization during post-processing.

The time synchronization process involves first truncating the longer IMU signal, either from the Piksi Multi system or the cadence system, to match the length of the shorter signal. Next, the signals are shifted in time relative to each other, and for each time shift, the error between the two signals is computed as the Euclidean norm of their difference. The optimal time shift is then determined by identifying the shift that results in the lowest error.

Figure 3.1 illustrates the time synchronization process, where the upper plot displays the initial unsynchronized gyroscope data, and the lower plot presents the synchronized signals following the applied procedure. The time synchronization process was implemented in Python, ensuring precise alignment between the two independent measurement systems. The synchronization methodology is based on the approach used by Moore (2012).

Time Synchronization Process

Unsynchronized IMU data

Synchronized IMU data
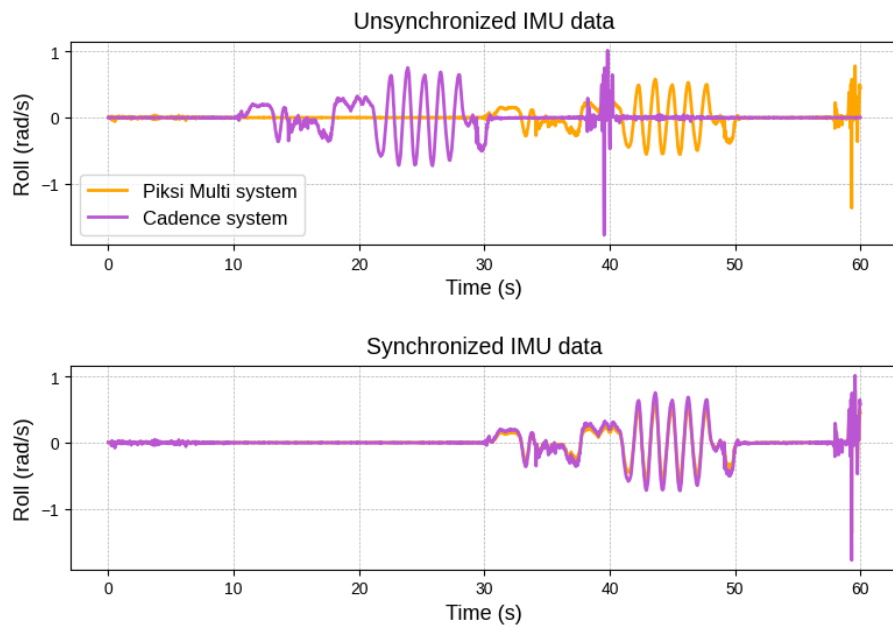
Figure 3.1: Illustration of the time synchronization process for the Piksi Multi system and the cadence system, based on their respective IMU gyroscope data. The top panel displays the gyroscope signals prior to synchronization, while the bottom panel presents the synchronized signals after applying the synchronization procedure. A time shift of 19.74 seconds was identified as optimal.

As a result of the synchronization procedure, data from the Piksi Multi system and the cadence system can be seamlessly integrated, as both systems now operate within a shared timeframe. This process only ensures synchronization between the two independent systems mounted on a single bicycle. Since the objective of this study is to analyze interactions between two cyclists, synchronization across both bicycles is also required. However, as both Piksi Multi systems operate on high-precision GPS time, no additional synchronization steps are necessary. The timestamps recorded by the Piksi Multi systems on both bicycles are inherently aligned, enabling direct comparison of the data collected from the two cyclists without requiring further adjustments.

<div style="text-align: right; font-size: 4em;">4</div>
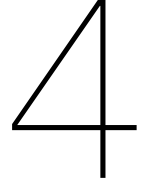
Kinematic Analysis

Following the data collection and processing methodologies detailed in preceding chapters, this chapter presents the kinematic data analysis designed to address the first research question. The analysis is organized into six sections. The initial two sections focus on the analysis of position data, while sections three, four, and five examine velocity data. The concluding section outlines the methodology used to analyze avoidance strategies, which involved classifying path adjustments and velocity modifications across various encounter scenarios and evaluating their interdependence.

4.1. Path adjustment metric

To quantify cyclist path adjustments, average orthogonal deviation was selected as the primary metric. This measure offers a robust representation of trajectory behavior by capturing deviations across the entire interaction segment, rather than focusing on isolated extremes. By accounting for the accumulation of small, consistent deviations, it offers a more comprehensive and nuanced assessment of path variability. The metric was computed by taking the mean of the perpendicular distances between each point on the interaction trajectory and the corresponding points on a reference trajectory. Since each participant has two reference trajectories, this calculation was performed separately for both, yielding two average deviation values. The computation is represented by the following equations:

$$P_{\text{int1},k} = \frac{1}{N} \sum_{i=1}^{N} |d_{\text{int1},k,i}|$$

$$P_{\text{int2},k} = \frac{1}{N} \sum_{i=1}^{N} |d_{\text{int2},k,i}|$$

(4.1)

In these equations, $P_{\text{int1},k}$ represents the average orthogonal deviation between the first reference trajectory and the interaction trajectory for a participant in trial k, where $1 \leq k \leq 8$. Likewise, $P_{\text{int2},k}$ denotes the average orthogonal deviation relative to the second reference trajectory. The term $|d_{\text{int1},k,i}|$ denotes the absolute orthogonal distance from the i-th point on the first reference trajectory to the corresponding point on the interaction trajectory. Since $d_{\text{int1},k,i}$ can take positive or negative values depending on the direction of deviation, information not considered in this part of the analysis, the absolute value is used. To ensure a consistent geometric basis for computing $P_{\text{int1},k}$ and $P_{\text{int2},k}$, all perpendicular distances were calculated by projecting points from the reference trajectories onto the respective comparison trajectories.

To ensure consistency across trials, the number of points N was standardized to 100 by interpolating the coordinates within the semi-circle to equally spaced points. This interpolation density was empirically determined to be sufficient. An analysis of the participant with the longest trajectory confirmed that the average orthogonal deviation stabilized beyond 100 points, with no appreciable changes observed

at higher resolutions. This normalization step facilitates direct comparison of trajectories independent of individual cycling speed.

Similarly, for each participant, the average orthogonal deviation between the first and second reference trajectories in trial k was calculated using the following equation:

$$P_{\text{ref},k} = \frac{1}{N} \sum_{i=1}^{N} |d_{\text{ref},k,i}| \qquad (4.2)$$

In this equation, $|d_{\text{ref},k,i}|$ denotes the perpendicular distance from the i-th point on the first reference trajectory to the second reference trajectory in trial k. All perpendicular distances were calculated by projecting points from the first reference trajectory onto the second reference trajectory.

Figure 4.1 illustrates the computation of $P_{\text{int1},k}$ and $P_{\text{ref},k}$. For visual clarity, only 20 dashed lines are shown to represent the orthogonal distances $d_{\text{int1},k,i}$ and $d_{\text{ref},k,i}$, rather than displaying the full set of 100.
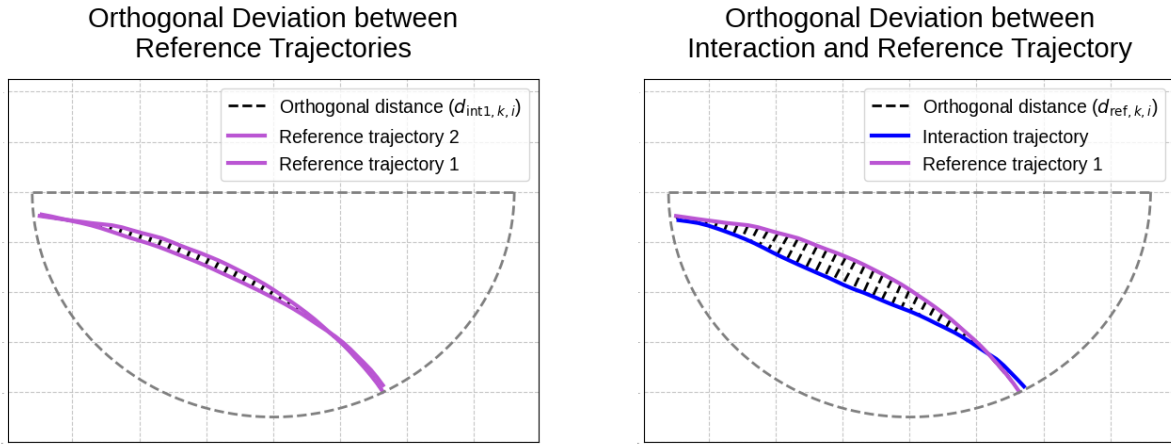
Figure 4.1: Illustration of orthogonal deviation. The left panel visualizes the orthogonal distances between two reference trajectories. The right panel depicts the orthogonal distances between the reference and interaction trajectory. The orthogonal distances, indicated by *black dashed lines*, are summed and averaged to compute the average orthogonal deviation. The *grey dashed line* represents the semi-circular arrangement.

Subsequently, $P_{\text{int1},k}$ and $P_{\text{int2},k}$ were compared to $P_{\text{ref},k}$ across all participants for each of the eight trials. This comparison aimed to assess whether path adjustments observed in interaction scenarios differed significantly from those in non-interaction scenarios.

4.1.1. Analysis

For the analysis of average orthogonal deviation, the data were organized into 16 distinct datasets. These included eight interaction scenarios, each comprising 20 observations of $P_{\text{int1},k}$ corresponding to the 20 participants. Similarly, the dataset included eight non-interaction scenarios, each containing 20 observations of $P_{\text{ref},k}$.

A one-way repeated measures ANOVA was chosen for the analysis, as the repeated measures design involved each participant contributing data across all eight trials in both conditions. The primary objective was to determine whether average orthogonal deviation differed significantly between interaction and non-interaction scenarios. In addition, separate analyses were conducted to assess differences among the interaction scenarios and among the non-interaction scenarios. Accordingly, three one-way repeated measures ANOVAs were performed.

When a large proportion of the 16 datasets exhibit substantial deviations from normality, repeated mea-

sures ANOVA may not be the optimal statistical test. The Shapiro-Wilk test, a statistical test appropriate for small datasets, was used to evaluate the normality of the data distributions (King & Eckersley, 2019; Shapiro & Wilk, 1965). The test evaluates the conformity of the sorted sample values to a normally distributed population, calculating the test statistic, W, as follows:

$$W = \frac{\left(\sum_{i=1}^{n} a_i x_{(i)}\right)^2}{\sum_{i=1}^{n}(x_i - \bar{x})^2} \tag{4.3}$$

In this equation, $x_{(i)}$ denotes the i-th order statistic, meaning the i-th smallest value in the sample after sorting the data in ascending order. In contrast, x_i refers to the i-th value in the original dataset. The term $\bar{x}$ represents the sample mean. The constants a_i are weights that reflect how a sample from a normal distribution is expected to behave when sorted. These weights are calculated based on the expected values and covariances of the order statistics from a standard normal distribution (Shapiro & Wilk, 1965). The sample size, n, was 20, indicating the number of observations per dataset. The resulting W statistic quantifies the degree of normality, with values closer to 1 indicating a stronger fit to the normal distribution.

The Shapiro-Wilk tests revealed that 3 out of 16 datasets deviated from normality. Although this finding could raise concerns about the validity of ANOVA, this method is recognized for its robustness to moderate violations of normality, especially within repeated measures designs (Ito, 1980). Consequently, ANOVA was deemed appropriate for this analysis.

Following the three separate one-way repeated measures ANOVAs, post-hoc pairwise comparisons were conducted to explore specific differences. Given that 3 out of 18 datasets exhibited deviations from normality, the Wilcoxon signed-rank test was used for post-hoc analyses. While ANOVA is robust to normality violations due to its analysis of global patterns, pairwise comparisons in post-hoc tests are susceptible to skewing from slight deviations. Therefore, the Wilcoxon signed-rank test, which does not assume normality, was chosen to ensure the validity of post-hoc inferences (Wilcoxon, 1945).

Pairwise testing within the interaction scenarios yielded 28 comparisons. Similarly, pairwise testing within the non-interaction scenarios resulted in 28 comparisons. A Bonferroni correction, dividing the significance level of $\alpha = 0.05$ by 28, produced an adjusted significance level of $\alpha = 0.0018$ (Dunn, 1961). Pairwise comparisons between interaction and non-interaction scenarios involved eight tests, leading to an adjusted significance level of $\alpha = 0.0063$.

It is important to note that the primary analysis presented in the main body of the thesis is based on comparisons between $P_{\text{int1},k}$ and $P_{\text{ref},k}$. A parallel analysis comparing $P_{\text{int2},k}$ and $P_{\text{ref},k}$ was also conducted, with the results presented in Appendix C.

4.2. Path adjustment correlation

To investigate correlations in path adjustments between interacting cyclists, paired average orthogonal deviation values ($P_{\text{int1},M1}, P_{\text{int1},M2}$) were compiled into a dataset. The index M ($1 \leq M \leq 10$) denotes each of the 10 cyclist pairs in the study, while the subscript identifies the individual cyclist within the pair. The direction of each cyclist's path adjustment is defined by the sign of $P_{\text{int1},M1}$ and $P_{\text{int1},M2}$. Due to the smooth nature of the trajectories, this direction is determined by the sum of signed orthogonal distances. For instance, if $\sum d_{\text{int1},k,i} = -2$, the sign of $P_{\text{int1},M1}$ is assigned as negative. An example of a negative average orthogonal deviation is shown in Figure 4.1. To ensure consistent ordering, data were structured such that $P_{\text{int1},M1} > P_{\text{int1},M2}$ within each pair. This ordering facilitates the computation of the Pearson correlation coefficient, using the following formula:

$$r = \frac{\sum_{M=1}^{10} \left(P_{\text{int1},M1} - \overline{P}_{\text{int1}}\right)\left(P_{\text{int1},M2} - \overline{P}_{\text{int2}}\right)}{\sqrt{\sum_{M=1}^{10} \left(P_{\text{int1},M1} - \overline{P}_{\text{int1}}\right)^2} \cdot \sqrt{\sum_{M=1}^{10} \left(P_{\text{int1},M2} - \overline{P}_{\text{int2}}\right)^2}} \tag{4.4}$$

Here, $\overline{P}_{\text{int1}}$ and $\overline{P}_{\text{int2}}$ represent the mean average orthogonal deviations for the cyclist in each pair with the larger and smaller path adjustment, respectively, calculated across all 10 pairs and 8 trials. This dataset, totaling 80 observations, served as the basis for the correlation analysis.

While the Pearson correlation coefficient provides insight into the directional relationship between cyclists' path adjustments, it does not capture differences in magnitude. To address this, a path adjustment ratio was computed for each cyclist pair in the four encounter scenarios, defined as:

$$\text{Path adjustment ratio}_{M,s} = |P_{\text{int1},M1,s}| : |P_{\text{int1},M2,s}| \tag{4.5}$$

where s represents the encounter scenario, and the values are ordered such that $|P_{\text{int1},M1}| < |P_{\text{int1},M2}|$. Unlike the correlation coefficient, which considers directionality, the adjustment ratio focuses exclusively on the magnitude of deviation by using absolute values. By normalizing $|P_{\text{int1},M1}|$ and $|P_{\text{int1},M2}|$ with respect to $|P_{\text{int1},M1}|$, the path adjustment ratio is defined as:

$$\text{Path adjustment ratio}_{M,s} = 1 : X \tag{4.6}$$

For each scenario s, 20 path adjustment ratios were computed. Differences in these ratios across scenarios were examined using a one-way repeated measures ANOVA.

By incorporating both the Pearson correlation coefficient and the adjustment ratio, the analysis provides a more comprehensive understanding of both the direction and magnitude of path adjustments during interactions.

4.3. Velocity metric

Examination of the velocity data showed that participants exhibited a relatively stable velocity throughout the experimental period. Based on this observation, average velocity was chosen as the primary metric. It is acknowledged that using average velocity could have resulted in the loss of valuable information if substantial velocity variations had been present.

Prior to computing the average velocity, a second-order low-pass Butterworth filter with a cutoff frequency of 2 Hz was applied to the raw velocity data. To facilitate the detection of high-acceleration hard braking maneuvers, the cutoff frequency was deliberately set to a value above the typical cycling frequency, which is generally below 1.5 Hz (Al-Naime et al., 2020). The effect of Butterworth filtering on raw velocity data is illustrated in detail in Appendix B.

The average velocity for each participant in trial k was calculated as:

$$v_{\text{int},k} = \frac{1}{N} \sum_{i=1}^{N} v_{\text{int},i} \tag{4.7}$$

where $v_{\text{int},i}$ represents the velocity at sample point i. N represents the number of data points within the trial, which may vary between participants and across trials. Similarly, the average velocities for each participant's two reference trajectories were computed using the following equations:

$$v_{\text{ref1},k} = \frac{1}{N} \sum_{i=1}^{N} v_{\text{ref1},i}$$

$$\tag{4.8}$$

$$v_{\text{ref2},k} = \frac{1}{N} \sum_{i=1}^{N} v_{\text{ref2},i}$$

Here, $v_{\text{ref1},i}$ and $v_{\text{ref2},i}$ denote the velocities at sample point i for the first and second reference trajectories, respectively. Subsequently, $v_{\text{int},k}$ was compared to both $v_{\text{ref1},k}$ and $v_{\text{ref2},k}$ across all participants and for each of the eight trials. This comparison aimed to evaluate whether average velocities during interaction scenarios differed significantly from those observed in non-interaction scenarios.

4.3.1. Analysis

Consistent with the path adjustment analysis presented in Subsection 4.1.1, the investigation of velocity selection modifications employed the same statistical framework. The Shapiro–Wilk test indicated that only 1 out of the 16 datasets deviated from normality, supporting the suitability of ANOVA for the analysis.

The primary objective of this analysis was to determine whether average velocity differed significantly between interaction and non-interaction scenarios. Additionally, separate analyses were conducted to examine differences among the interaction scenarios and among the non-interaction scenarios. Accordingly, three one-way repeated measures ANOVAs were performed. For post-hoc comparisons, Wilcoxon signed-rank tests were conducted, followed by a Bonferroni correction to control for multiple comparisons.

It is important to note that the primary analysis presented in the main body of the thesis is based on comparisons between $v_{\text{int},k}$ and $v_{\text{ref1},k}$. A parallel analysis comparing $v_{\text{int},k}$ and $v_{\text{ref2},k}$ was also conducted, with the results presented in Appendix D.

4.4. Velocity selection correlation

Expanding upon the path adjustment correlation analysis, this study also examines the relationship between the velocity selections of interacting cyclists. The aim is to determine whether a reduction in velocity by one cyclist corresponds to an increase in velocity by the other, indicating potential reciprocal behavior. To quantify this relationship, the absolute difference between the average velocity of the interaction trajectory and that of the first reference trajectory was calculated for each participant and trial. The same procedure was repeated for the second reference trajectory. This relationship is expressed as follows:

$$\Delta v_{\text{int1},k} = v_{\text{int},k} - v_{\text{ref1},k}$$
$$\Delta v_{\text{int2},k} = v_{\text{int},k} - v_{\text{ref2},k}$$

(4.9)

$\Delta v_{\text{int1},k}$ represents the difference in average velocity between the first reference trajectory and the interaction trajectory for a participant in trial k. $\Delta v_{\text{int2},k}$ denotes the difference in average velocity between the second reference trajectory and the interaction trajectory. $v_{\text{int},k}$ and $v_{\text{ref},k}$ denote the average velocity of the participant in trial k for the interaction and reference trajectories, respectively.

For the investigation of velocity selection correlations between interacting cyclists, paired difference in average velocity data, $(\Delta v_{\text{int1},M1}, \Delta v_{\text{int1},M2})$, was structured into a dataset. The index M ($1 \leq M \leq 10$) represents each cyclist pair, indicating the 10 pairs that constituted the study cohort. The numerical subscript denotes the specific cyclist within each pair. To ensure consistency and avoid arbitrary ordering effects, the data was systematically arranged such that $\Delta v_{\text{int1},M1} > \Delta v_{\text{int1},M2}$ for each pair. This facilitates the calculation of the Pearson correlation coefficient via the subsequent formula:

$$r = \frac{\sum_{M=1}^{10} \left(\Delta v_{\text{int1},M1} - \overline{\Delta v}_{\text{int1}} \right) \left(v_{\text{int1},M2} - \overline{\Delta v}_{\text{int2}} \right)}{\sqrt{\sum_{M=1}^{10} \left(\Delta v_{\text{int1},M1} - \overline{\Delta v}_{\text{int1}} \right)^2} \cdot \sqrt{\sum_{M=1}^{10} \left(\Delta v_{\text{int1},M2} - \overline{\Delta v}_{\text{int2}} \right)^2}}$$

(4.10)

Here, $\overline{\Delta v}_{\text{int1}}$ and $\overline{\Delta v}_{\text{int2}}$ represent the mean differences in average velocities for the cyclist in each pair with the larger and smaller magnitudes of velocity changes, respectively, calculated across all 10 pairs and 8 trials. This dataset, totaling 80 observations, served as the basis for the correlation analysis.

Negative values of $\Delta v_{\text{int1},M1}$ and $\Delta v_{\text{int1},M2}$ indicate that participants selected a lower velocity in interaction scenarios compared to non-interaction scenarios, whereas positive values indicate that participants increased their velocity during interactions.

In addition to examining the directional relationship, the velocity selection ratio was calculated for each cyclist pair to quantify the relative magnitude of velocity adjustments during interaction. This ratio is defined as:

$$\text{Velocity adjustment ratio}_{M,s} = |\Delta v_{\text{int1},M1,s}| : |\Delta v_{\text{int1},M2,s}| \tag{4.11}$$

Velocity selection ratios were determined for interacting cyclists in pair M within each of the four encounter scenarios s. These adjustments are represented by the difference in average velocity $\Delta v_{\text{int1},M1,s}$ and $\Delta v_{\text{int1},M2,s}$, organized such that $|\Delta v_{\text{int1},M1,s}| < |\Delta v_{\text{int1},M2,s}|$. By normalizing $|\Delta v_{\text{int1},M1,s}|$ and $|\Delta v_{\text{int1},M2,s}|$ with respect to $|\Delta v_{\text{int1},M1,s}|$, the path adjustment ratio is defined as:

$$\text{Velocity selection ratio}_{M,s} = 1 : Y \tag{4.12}$$

For each encounter scenario s, a total of 20 velocity adjustment ratios were calculated, based on data from 10 cyclist pairs, each completing two trials. Differences in these ratios across scenarios were examined using a one-way repeated measures ANOVA.

4.5. Braking and acceleration patterns

The previous section examined the selected velocities of participants across different scenarios, focusing on average velocities. However, analyzing average velocities alone may overlook critical dynamic aspects of participant behavior. To gain a more comprehensive understanding, this analysis evaluates individual variations in acceleration profiles. Average absolute acceleration was selected as a key metric to quantify the intensity of speed fluctuations throughout each trial. By taking the absolute value of acceleration, both increases and decreases in velocity contribute positively to the measure, avoiding cancellation effects that can occur with net acceleration. This ensures that even subtle variations in speed are captured.

Acceleration was calculated from the Butterworth-filtered velocity data acquired from the Piksi Multi system. The average absolute acceleration for trial k was computed by summing the absolute acceleration values of the participant's trajectory, as defined by the following equation:

$$a_{\text{int},k} = \frac{1}{N} \sum_{i=1}^{N} \left| \frac{v_{\text{int},i+1} - v_{\text{int},i}}{\Delta t} \right| \tag{4.13}$$

$v_{\text{int},i}$ represent the velocity at point i, and Δt is the constant sampling interval of 0.1 seconds. N represents the length of each participant's dataset for each trial, which varies due to differing velocity dataset lengths.

Similarly, the absolute average acceleration for each participant in each of the two reference trajectories was calculated as follows:

$$a_{\text{ref1},k} = \frac{1}{N} \sum_{i=1}^{N} \left| \frac{v_{\text{ref},i+1} - v_{\text{ref},i}}{\Delta t} \right|$$

$$a_{\text{ref2},k} = \frac{1}{N} \sum_{i=1}^{N} \left| \frac{v_{\text{ref},i+1} - v_{\text{ref},i}}{\Delta t} \right| \tag{4.14}$$

Subsequently, $a_{\text{int},k}$ was compared to $a_{\text{ref1},k}$ and $a_{\text{ref2},k}$ across all participants for each of the eight trials. This comparison sought to determine whether acceleration patterns in interaction scenarios were significantly different from those in non-interaction scenarios.

4.5.1. Analysis
Consistent with the path adjustment and velocity selection analysis described in Subsection 4.1.1 and 4.3.1, the analysis of braking and acceleration patterns followed the same statistical approach. The Shapiro-Wilk test indicated that 4 out of 16 datasets deviated from normality, supporting the suitability of ANOVA for the analysis.

Three separate one-way repeated measures ANOVAs were conducted to determine whether average absolute acceleration differed significantly between interaction and non-interaction scenarios across all eight trials, and to explore differences among interaction scenarios and among non-interaction scenarios separately. Accordingly, three one-way repeated measures ANOVAs were performed. For post-hoc comparisons, Wilcoxon signed-rank tests were conducted, followed by a Bonferroni correction to control for multiple comparisons.

It is important to note that the primary analysis presented in the main body of the thesis is based on comparisons between $a_{\text{int},k}$ and $a_{\text{ref1},k}$. A parallel analysis comparing $a_{\text{int},k}$ and $a_{\text{ref2},k}$ was also conducted, with the results presented in Appendix E.

4.6. Avoidance strategies
The methodology for computing path adjustment and velocity selection metrics was presented in prior sections. However, the operational definitions for classifying these actions as significant adjustments or modifications were not specified. This section addresses this gap by defining these criteria. It then proceeds to describe the framework used to define and analyze collision avoidance strategies across the four encounter scenarios.

4.6.1. Classification criteria
In this study, a path adjustment was identified when both $P_{\text{int1},k}$ and $P_{\text{int2},k}$ for each participant and trial k exceeded a threshold. This threshold was defined as the mean of all $P_{\text{ref},k}$ values across all participants and trials k, plus one standard deviation (σ). Thus, a path adjustment was deemed significant when:

$$\text{Path adjustment} = \min(P_{\text{int1},k}, P_{\text{int2},k}) > \overline{P}_{\text{ref}} + \sigma_{P_{\text{ref}}}$$
$$\text{Path adjustment} = \min(P_{\text{int1},k}, P_{\text{int2},k}) > 0.25 + 0.09 \tag{4.15}$$

As evident from Equation 4.15, cyclists exhibiting an average orthogonal deviation from their reference trajectories exceeding 0.34 m were classified as having adjusted their path. The rationale for this threshold methodology stems from the observed smoothness of path trajectories and the infrequent occurrence of sharp evasive maneuvers. The threshold was established to account for natural variability among cyclists, thereby reducing the likelihood of false positives while avoiding excessively conservative cutoffs. This approach offers a balanced and interpretable means of differentiating normal trajectory variability from intentional path adaptations during interactions.

Figure 4.2 visually demonstrates the criteria for classifying path adjustments. The two small dashed lines in each subplot illustrate the threshold used for this classification. It is important to clarify that this figure is intended for visualization purposes only, as the threshold in this study is a single numerical value, not a continuous line. The aim is to provide an intuitive understanding of the magnitude of path adjustments that are considered significant.
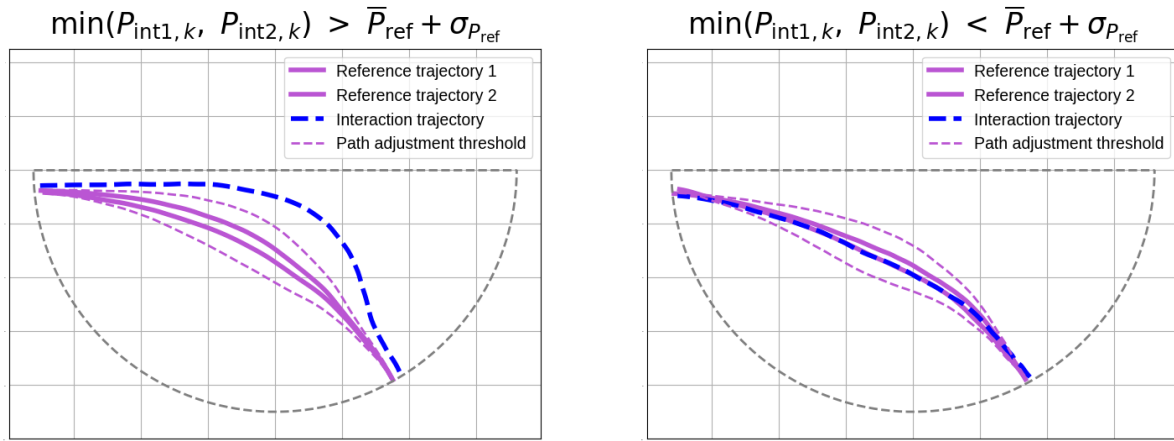
Figure 4.2: Visual depiction of how a path adjustment is defined. In the left subplot, the participant is classified as having adjusted their path during interaction with another cyclist. In the right subplot, the participant is not classified as having adjusted their path in the interaction scenario.

Similarly, a cyclist's velocity selection was classified as modified when both $|\Delta v_{\text{int1},k}|$ and $|\Delta v_{\text{int2},k}|$ exceeded a predefined threshold. To determine this threshold, the absolute difference in average velocities between the two reference trajectories was first calculated for each participant in every trial, as follows:

$$\Delta v_{\text{ref},k} = |v_{\text{ref1},k} - v_{\text{ref2},k}| \tag{4.16}$$

The threshold was subsequently determined by computing the mean of $\Delta v_{\text{ref},k}$ across all trials and adding one standard deviation (σ). This relationship is expressed mathematically as:

$$\text{Velocity selection} = \min(|\Delta v_{\text{int1},k}|, |\Delta v_{\text{int2},k}|) > \Delta \overline{v}_{\text{ref}} + \sigma_{\Delta v_{\text{ref}}}$$
$$\text{Velocity selection} = \min(|\Delta v_{\text{int1},k}|, |\Delta v_{\text{int2},k}|) > 0.15 + 0.066 \tag{4.17}$$

As evident from Equation 4.17, if cyclists exhibited a modified velocity selection exceeding 0.216 m/s compared to their reference trajectory, the cyclist was classified as having modified their selected velocity. A visual representation of this classification is provided in Figure 4.3. It is crucial to clarify that this figure serves only for visualization, as the threshold is a single numerical value, not a continuous line. The aim is to provide an intuitive understanding of the magnitude of velocity selections considered significant.

Figure 4.3: Visual illustration of the criteria used to define a modified velocity selection. The left subplot demonstrates a participant classified as having altered their velocity selection, in contrast to the right subplot, which shows a participant not classified as having made such a change.

4.6.2. Analysis

The final analysis aimed to assess the relationship between collision avoidance strategies and encounter scenarios. For each encounter scenario, the collision avoidance strategy imp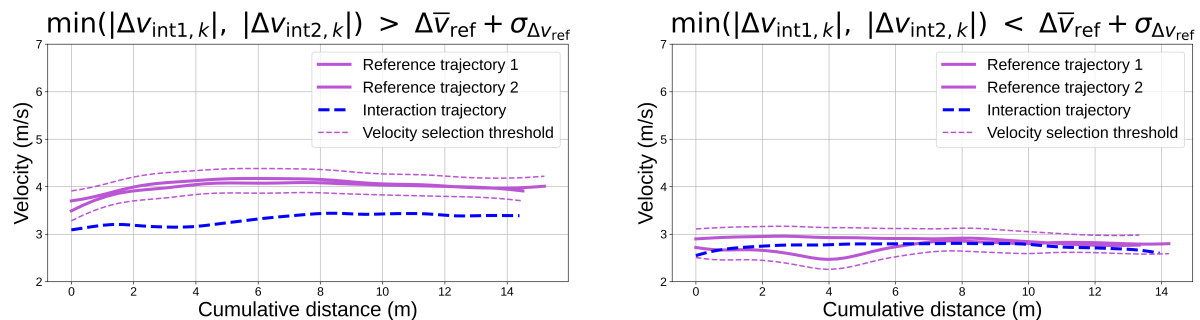lemented by each cyclist pair was identified, yielding 10 possible strategy combinations. Each cyclist could perform one of four actions: combined path adjustment and velocity selection modification (PA & VS), path adjustment alone (PA), velocity selection modification alone (VS), or no adjustment (NO). The frequency of each strategy combination within each encounter scenario was then compiled into a contingency table, as shown in Figure 4.4.

Figure 4.4: Empty contingency table displaying the frequency of avoidance strategies, categorized by the four different encounter scenarios. Although the table initially contains only zeros, it will later be populated with the observed counts for each avoidance strategy. For instance, the column labeled 'PA & VS, PA & VS' indicates instances where both cyclists in a pair modified both their path and velocity.

After populating the contingency table with the observed counts of each collision avoidance strategy across the different encounter scenarios, a Chi-square test was conducted. The observed frequencies, O_{ij}, reflecting the actual strategy choices, were arranged based on the four encounter scenarios (i) and the ten strategy categories (j). The Chi-Square test then calculates the expected frequencies, E_{ij}, under the null hypothesis of uniform strategy distribution across the four scenarios. E_{ij} is calculated as follows:

$$E_{ij} = \frac{(\text{Row Total}_i) \cdot (\text{Column Total}_j)}{\text{Grand Total}} \tag{4.18}$$

where Row Total$_i$ equals 20, representing 10 cyclist pairs completing 2 trials per encounter scenario, and Grand Total equals 80. Subsequently, the deviation of each observed frequency (O_{ij}) from the expected frequency (E_{ij}) was calculated using the following formula:

$$\chi^2 = \sum_{i=1}^{4} \sum_{j=1}^{10} \frac{(O_{ij} - E_{ij})^2}{E_{ij}} \tag{4.19}$$

A large χ^2 means there is a large difference between the observed frequencies O_{ij} and the expected frequencies E_{ij} under the null hypothesis of independence.

It is important to note that a significant Chi-Square test result indicates an association between scenario and avoidance strategy, but does not specify which scenarios differ. To identify specific differences, pairwise Chi-Square tests are required. A Bonferroni correction was applied, adjusting the significance threshold by dividing the conventional α level by the six pairwise comparisons.

5

Yielding

To examine the interaction characteristics that influence yielding behavior, a statistical model was developed to estimate the probability of yielding. This chapter first provides a detailed discussion of the factors included in the analysis, along with the rationale for their selection. Next, the potential impact of collinearity among model variables is assessed to ensure the reliability of the statistical estimates. The chapter concludes with an overview of the model selection process and an evaluation of the model's predictive performance.

5.1. Model variables

As previously stated, the primary objective of the model is to estimate the probability of yielding. In this study, yielding is defined as the behavior of a cyclist who, in a close interaction with another cyclist, crosses the intersection last as a result of a priority resolution process. However, this definition may also include passages where neither cyclist adjusts their motion, rather than true interactions that involve active yielding. Some interactions may instead be classified as passages, where the cyclist crossing last is merely arriving later rather than actively yielding (Haperen et al., 2018). A passage, as defined in this study, occurred when both cyclists in the interacting pair did not adjust their path or modify their selected velocity, based on the classification criteria outlined in Subsection 4.6.1.

Yielding behavior is determined based on position data from the Piksi Multi system, which provides precise timestamps for each cyclist's trajectory. At the intersection point where their paths cross, the timestamps of the interacting cyclists are compared. The cyclist with the later timestamp is identified as the one who yields. In the statistical model, yielding is designated as the dependent variable and is represented as a binary outcome, capturing the presence or absence of yielding behavior.

The independent variables in this study were selected based on prior research, focusing on factors presumed to influence yielding behavior. These variables were chosen to ensure a consistent predictive horizon across all predictors. In this study, the predictive horizon is defined as the point at which cyclists enter the semi-circle, representing the spatial context in which yielding decisions are made. This approach ensures that predictions are based on a standardized reference point rather than varying temporal intervals, as the time elapsed between cyclists entering the semi-circle and their paths intersecting differs for each interacting pair.

The first factor analyzed is the difference in time to arrival (DTA), which quantifies the temporal disparity between cyclists as they approach the semi-circle. Previous research by Mohammadi et al. (2023) has identified DTA as a significant predictor of yielding behavior in cyclist-vehicle interactions, suggesting that this metric may also be relevant in cyclist-cyclist interactions. DTA is derived from position data by examining the timestamps at which cyclists enter the semi-circle. For example, if one cyclist arrives 0.3 seconds earlier than another, the earlier cyclist has a DTA of +0.3 seconds, while the later cyclist has a DTA of -0.3 seconds. A negative DTA, therefore, indicates that a cyclist arrives later than their interacting counterpart.

Additionally, Mohammadi et al. (2023) demonstrated that the initial velocities of both vehicles and cyclists significantly influence yielding decisions. To assess the relevance of this factor in cyclist-cyclist interactions, the initial velocity difference was included as a variable in this study. While participants were instructed to maintain a constant velocity of 10 km/h upon entering the semi-circle, data analysis revealed that velocity differences were still present, underscoring the importance of accounting for these variations. For example, if two interacting cyclists have initial velocities of 2.9 m/s and 2.7 m/s, respectively, the first cyclist would have an initial velocity difference of +0.2 m/s, while the second cyclist would have an initial velocity difference of -0.2 m/s. Similar to DTA, initial velocity differences were computed using velocity data sourced directly from the Piksi Multi system.

This study pairs male and female participants to examine potential gender differences in yielding behavior. Gender information was collected through a pre-study questionnaire. In addition to considering gender as a potential predictor of yielding behavior, this study investigates the direction of approach to the semi-circle as a factor that may influence yielding decisions. Previous research has indicated that cyclists often follow informal traffic norms, even in areas where explicit traffic regulations are absent (Wexler & El-Geneidy, 2017). Building on this hypothesis, the perceived approach direction is expected to influence yielding behavior. In the Netherlands, traffic regulations mandate that road users approaching from the right have the right of way. Based on this rule, it is hypothesized that cyclists approaching from the left are more likely to yield to those approaching from the right. This implies that cyclists in the 45^E, 90^F, 135^B, and 180^A scenarios may perceive themselves as the right-approaching cyclist.

Grigoropoulos et al. (2022) identified cadence, specifically the cessation of pedaling, as a potential factor influencing a cyclist's yielding behavior when interacting with motorized vehicles. In this research, they found that cyclists ceasing pedaling is an indicator of yielding when interacting with a motorized vehicle. Therefore, cessation of pedaling may also be a predictor in cyclist-cyclist interactions.

The final independent factor investigated was the encounter angle. However, the encounter angle itself was not a suitable predictor, as yielding occurred in 50% of observations within each encounter scenario. Consequently, incorporating this predictor would not enhance model fit or predictive capability, as it does not provide any signal to differentiate yielding behavior. The interaction between encounter angle and approach direction was, nevertheless, explored, recognizing that approach direction may have a more pronounced impact in specific encounter scenarios. Additionally, the interaction between DTA and initial velocity difference was examined to understand the dynamic evolution of relative positions. An overview of the independent variables is provided in Table 5.1.

Table 5.1: Overview of the independent factors included in the model. The first column lists the factors, while the second and third columns provide their types and descriptions, respectively.

Independent factor	Type	Description
DTA	Continuous	Represents the temporal difference between cyclists reaching the semi-circle. Cyclists who approach the semi-circle earlier exhibit a positive DTA, while those who arrive later have a negative DTA.
Gender	Binary	All participants in this study self-identified as either female or male. Gender was recorded as a binary variable, with 0 representing female and 1 representing male.
Initial velocity difference	Continuous	The initial velocity difference represents the relative velocity between participants at the moment they enter the semi-circle. A positive value indicates that the participant is moving faster than their interacting counterpart, whereas a negative value signifies that the participant is moving slower.
Approach direction	Binary	Participants starting from positions A, B, E, and F are classified as approaching from the right and are coded as 0, whereas those starting from positions C, D, G, and H are classified as approaching from the left and are coded as 1.
Cadence	Binary	At the onset of entering the semi-circle, participants' behavior is encoded as follows: a value of 0 indicates that the participant stopped pedaling, while a value of 1 indicates that the participant continued pedaling.
Encounter angle	Categorical	The four distinct approach angles, 45°, 90°, 135°, and 180°, were categorically represented by the numerical values 1, 2, 3, and 4, respectively.

5.2. Model collinearity

Collinearity in statistical modeling, particularly in regression analysis, occurs when two or more predictor variables exhibit a high degree of correlation (Dormann et al., 2012; Montgomery et al., 2010). Such relationships can compromise the model's ability to accurately estimate the individual effects of predictors, as the regression algorithm struggles to disentangle their shared contributions to the outcome variable.

To assess the potential presence of multicollinearity among predictor variables, the variance inflation factor (VIF) was calculated for each independent variable. The VIF quantifies the extent to which the variance of a regression coefficient is inflated due to collinearity with other predictors (Senter, 2008). Following standard guidelines, a VIF value below 5 was considered indicative of an acceptable level of collinearity, suggesting that the predictor variables did not exhibit substantial multicollinearity concerns (Montgomery et al., 2010).

5.3. Model selection

Yielding behavior was modeled as a binary outcome, thereby supporting the use of logistic regression for analysis. Given the repeated-measures design, where each participant completed eight trials, it was necessary to account for potential within-subject dependencies. Some individuals may exhibit consistent tendencies in their yielding behavior, with certain cyclists demonstrating a higher propensity to yield than others. To address the hierarchical structure of the data, the model incorporates random

effects at the participant level. This approach captures individual variability and adjusts for correlations within participants, thereby enhancing the accuracy and generalizability of the model's estimates.

The inclusion of random effects, and consequently the use of a multi-level model, requires careful evaluation to ensure their necessity. To select the most appropriate model, the influence of random effects is systematically assessed. This evaluation involves comparing the performance of a single-level logistic regression model with that of a multi-level logistic regression model to determine whether the additional complexity introduced by random effects is justified.

A logistic regression model assumes that the target variable follows a Bernoulli distribution, where it takes values of 0 (no yielding) or 1 (yielding). Rather than modeling probabilities directly, it models the log-odds of the outcome:

$$\log\left(\frac{p}{1-p}\right) = \beta_0 + \sum_{k=1}^{K} \beta_k x_k \tag{5.1}$$

where the left-hand side of the equation represents the log-odds of the binary outcome. On the right-hand side, β_0 denotes the intercept, representing the log-odds of the outcome when all predictor variables are set to zero, while β_k quantifies the effect of the kth predictor variable on the log-odds of the outcome. If β_k is not significantly different from zero, the corresponding predictor variable does not have a significant influence on the log-odds. The model can incorporate any number of predictor variables, denoted as K, to evaluate their combined effects on the binary outcome. Both β_0 and β_k are estimated using the Maximum Likelihood Estimation (MLE) method, which identifies the set of parameters that maximizes the likelihood of observing the given data under the specified model. This approach ensures that the estimated parameters provide the best fit to the data, effectively capturing the relationship between the predictor variables and the binary outcome.

Multi-level logistic regression models extend the single-level approach by incorporating random effects to account for hierarchical or nested data structures. This allows the model to capture variability among participants and their preferences for yielding. The relationship is represented as:

$$\log\left(\frac{p}{1-p}\right) = \beta_0 + \sum_{k=1}^{K} \beta_k x_k + u_i \tag{5.2}$$

where u_i represents the random intercept for participant i, modeling the variability in log-odds across participants. This term accounts for differences between participants and is assumed to follow a normal distribution, $u_i \sim \mathcal{N}(0, \sigma_u^2)$, with a mean of zero and variance σ_u^2.

After fitting both the single-level and multi-level models, the intraclass correlation coefficient (ICC) is calculated to assess the degree to which participants differ in their baseline tendencies to yield, after accounting for other predictors in the model. An ICC greater than 0.50 indicates that a substantial proportion of the variability in yielding behavior is attributable to differences between participants. In such cases, a multi-level model is more appropriate, as it accounts for this clustering and better captures the hierarchical structure of the data. Furthermore, a likelihood ratio test (LRT) is conducted to compare the fit of the two models. This test assesses whether the inclusion of random effects significantly enhances the model's fit. A p-value less than 0.05 indicates that the random effects are statistically significant and should be retained in the model.

To ensure consistency and facilitate model comparison, all statistical modeling was performed in R 4.4.2 (R Core Team, Vienna, Austria).

5.4. Model evaluation

The Akaike Information Criterion (AIC) and Bayesian Information Criterion (BIC) are widely recognized statistical tools for evaluating and comparing models, particularly in logistic regression and related fields. Both criteria assess the trade-off between model fit and complexity, penalizing models with excessive parameters to promote parsimony and mitigate the risk of overfitting. AIC, introduced by Akaike (1974), emphasizes predictive accuracy by estimating information loss, while BIC, proposed by Schwarz (1978), adopts a more conservative approach by incorporating the sample size into the penalty term, favoring simpler models in larger datasets. These criteria are complementary, providing robust insights into model selection for different goals, such as prediction or inference (Akaike, 1974; Schwarz, 1978).

Although AIC and BIC are valuable for evaluating model fit and complexity, assessing predictive performance is equally essential. Therefore, alternative models were implemented and evaluated alongside the model favored by AIC and BIC, ensuring a comprehensive comparison of their performance. It is important to highlight that if random effects are not warranted, indicating minimal variability between participants, the single-level and multi-level logistic regression models are expected to yield similar results.

To assess predictive accuracy, leave-one-out cross-validation (LOOCV) was employed. LOOCV is a rigorous cross-validation technique that is particularly well-suited for smaller datasets (Mohammadi et al., 2023). Given that this study's dataset consists of 160 observations, and datasets with fewer than 1000 observations are generally considered small, cross-validation is a recommended validation technique (Safonova et al., 2023). LOOCV ensures that every observation is used in the training process while also serving as a test case exactly once. This methodology maximizes the utility of the available data and provides a robust and comprehensive evaluation of the model's performance (Arlot & Celisse, 2010). In addition to employing LOOCV to compare statistical models, their performance was also evaluated against a baseline, such as a dummy classifier. A dummy classifier does not take independent variables into account but instead makes predictions for the target variable, yielding, solely based on the class distribution. In this study, the class distribution is perfectly balanced. However, with LOOCV, the model is trained 159 times, leaving out one observation in each iteration. As a result, the class distribution in each training set becomes slightly imbalanced. Comparing the statistical models to the dummy classifier allows for evaluating whether it offers a significant improvement in predictive power beyond random benchmarks (Bishop, 2007; Vehtari et al., 2016).

6

Kinematic Analysis Outcomes

This chapter presents the findings of the kinematic analysis introduced in Chapter 4, organized into four main sections. The first covers path parameters, including trajectory visualizations and average orthogonal deviations across scenarios. The second focuses on velocity, analyzing both overall distributions and scenario-specific averages. The third section examines the avoidance strategies used by interacting cyclist pairs and how these vary across the four encounter scenarios. Finally, the chapter concludes with an analysis of perceived comfort levels and their differences between scenarios.

6.1. Path analysis

This section analyzes path parameters, starting with trajectory plots for each encounter scenario. Subsequently, average orthogonal deviations are presented for each of the interaction and non-interaction scenarios.

6.1.1. Trajectory plots

Figure 6.1 illustrates the participants' trajectories, differentiating between interaction and non-interaction scenarios. As outlined in Chapter 4, interaction scenarios involve cyclists navigating the semi-circle while interacting with another cyclist, whereas non-interaction scenarios correspond to reference trajectories, in which participants cycled the track without the presence of another cyclist.

The non-interaction scenarios include 80 trajectories per subplot, derived from 20 cyclists, two travel directions, and two reference trajectories. In contrast, the interaction scenarios contain 40 trajectories per subplot, based on the same 20 cyclists and two travel directions, but with only a single interaction trajectory.

In order to compute the average trajectory among participants who traveled at varying speeds, each participant's data were parameterized by the distance traveled. First, the cumulative distance from the starting point was calculated for each participant. A common distance axis was then established, extending from zero up to the smallest maximum distance covered by any individual participant. Next, each participant's latitude and longitude measurements were interpolated onto this shared distance axis, thereby ensuring consistent alignment with respect to distance traveled. This procedure facilitated the straightforward calculation of average trajectories across all participants.

In addition to illustrating the average trajectory for each encounter scenario, Figure 6.1 includes light-shaded areas representing the standard deviation, capturing approximately 68% of the data distribution.

Trajectories for All Participants Across Scenarios
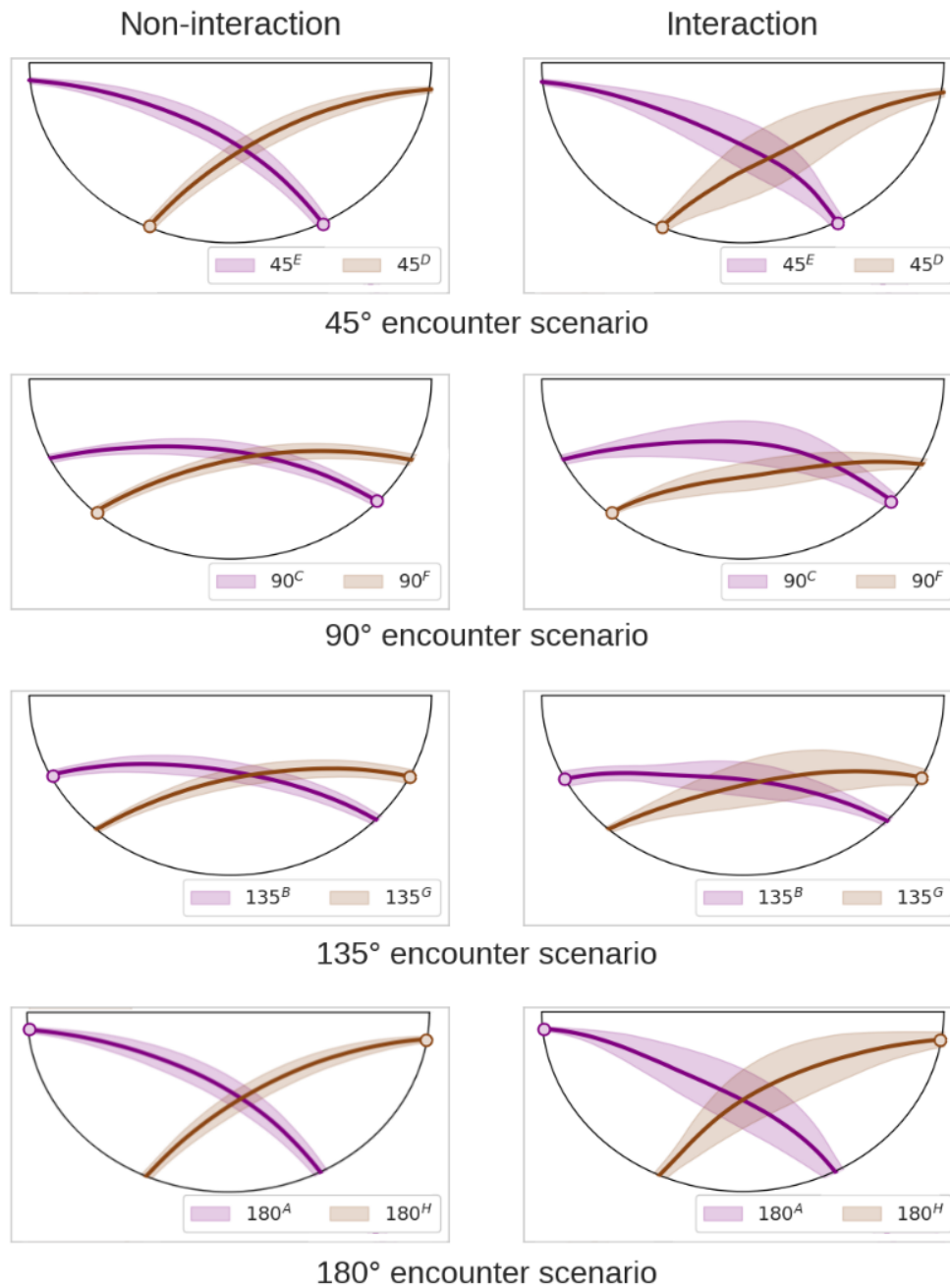
Figure 6.1: Mean trajectories of all participants, with standard deviations represented by shaded areas. *Solid lines* indicate the average trajectory for each group. The left column illustrates non-interaction scenarios, while the right column depicts interaction scenarios. The rows represent different encounter angles: 45°, 90°, 135°, and 180°. The *circles* denote the starting positions.

Figure 6.1 illustrates greater trajectory variability in interaction scenarios, as indicated by the broader shaded regions compared to those observed in non-interaction scenarios. The raw trajectory plots for each participant across the different scenarios, excluding the shaded regions, are presented in Appendix G.

Another noteworthy observation is that in both the 45° and 90° encounter scenarios, the point of intersection appears shifted to the right, potentially indicating that cyclists approaching from the right tend to cross first. However, this inference cannot be confirmed from the figure alone, as velocity is not

accounted for. In the 135° scenario, the intersection point remains consistent between interaction and non-interaction conditions. In contrast, the 180° scenario shows a leftward shift in the intersection point, which could suggest that cyclists in the 180^A condition generally cross first. However, this interpretation relies on the assumption of equal velocities and simultaneous entry into the semi-circle, conditions that were not examined in the present analysis.

6.1.2. Path adjustments

Figure 6.2 presents box plots comparing average orthogonal deviations between interaction and non-interaction scenarios.
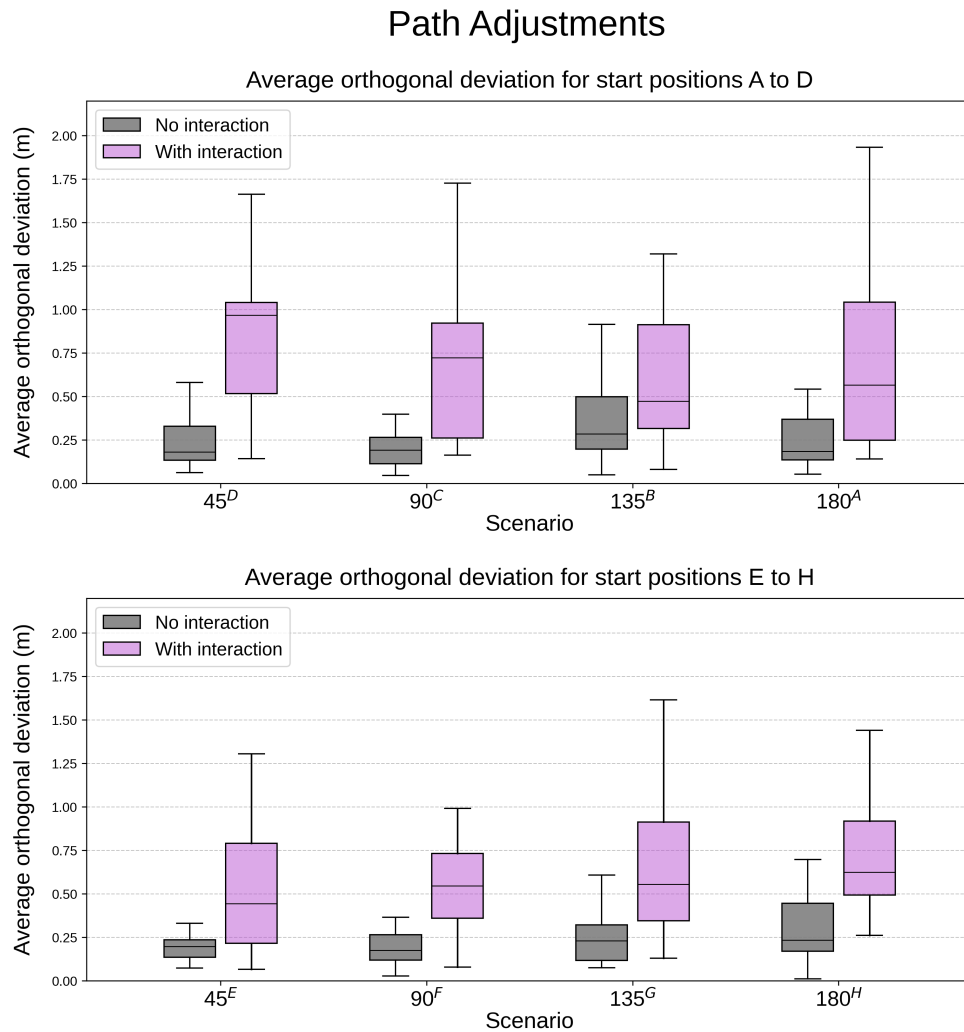
Figure 6.2: Box plots comparing path adjustments in interaction and non-interaction scenarios based on average orthogonal deviation. The upper plot represents trials where participants started on the left side of the semi-circle, while the lower plot represents trials where participants started on the right side. *Horizontal black lines* denote medians.

Figure 6.2 reveals that, based on the median, the most pronounced path adjustments occurred in the 45^D scenario, while the least pronounced adjustments were observed in the 135^B scenario. Additionally, interaction scenarios consistently exhibited greater average orthogonal deviations in participant trajectories compared to non-interaction scenarios. To assess the statistical significance of the observed differences in average orthogonal deviation, three separate one-way repeated measures ANOVAs were performed. The results of these analyses are presented in Table 6.1.

Table 6.1: Summary of results from three separate one-way repeated measures ANOVAs examining average orthogonal deviation across interaction and non-interaction scenarios.

ANOVA analysis	F (df$_1$, df$_2$)	P-value	η^2
Interaction scenarios	0.60 (7, 133)	0.76	0.030
Non-interaction scenarios	1.74 (7, 133)	0.11	0.084
Interaction vs non-interaction scenarios	58.04 (1, 19)	**0.0008**	0.75

According to Table 6.1, there were no significant differences in average orthogonal deviations within either the interaction or the non-interaction scenarios. In contrast, a significant difference was found between the interaction and non-interaction scenarios. The calculated η^2 of 0.75 represents a large effect size, signifying that 75% of the variance in average orthogonal deviation values is attributable to the difference between interaction and non-interaction scenarios.

Pairwise post-hoc comparisons revealed that in seven out of eight trials, with the exception of 135^B, the average orthogonal deviation was significantly greater in interaction scenarios compared to their non-interaction counterparts.

6.2. Velocity analysis

This section examines velocity, beginning with velocity plots for each encounter scenario. Subsequently, average velocities for both interaction and non-interaction conditions are presented. The section concludes with a detailed analysis of braking and acceleration patterns across the different scenarios.

6.2.1. Velocity plots

Figure 6.3 presents the velocity profiles for all participants, depicting horizontal velocity as a function of distance traveled. Consistent with the approach used in the trajectory plots, a standardized distance axis was established, ranging from zero to the shortest maximum distance covered by any participant. Each participant's velocity data was subsequently interpolated onto this shared distance axis to ensure comparability.

The shaded regions around each line in Figure 6.3, color-coded by condition, represent one standard deviation, encompassing approximately 68% of the data.
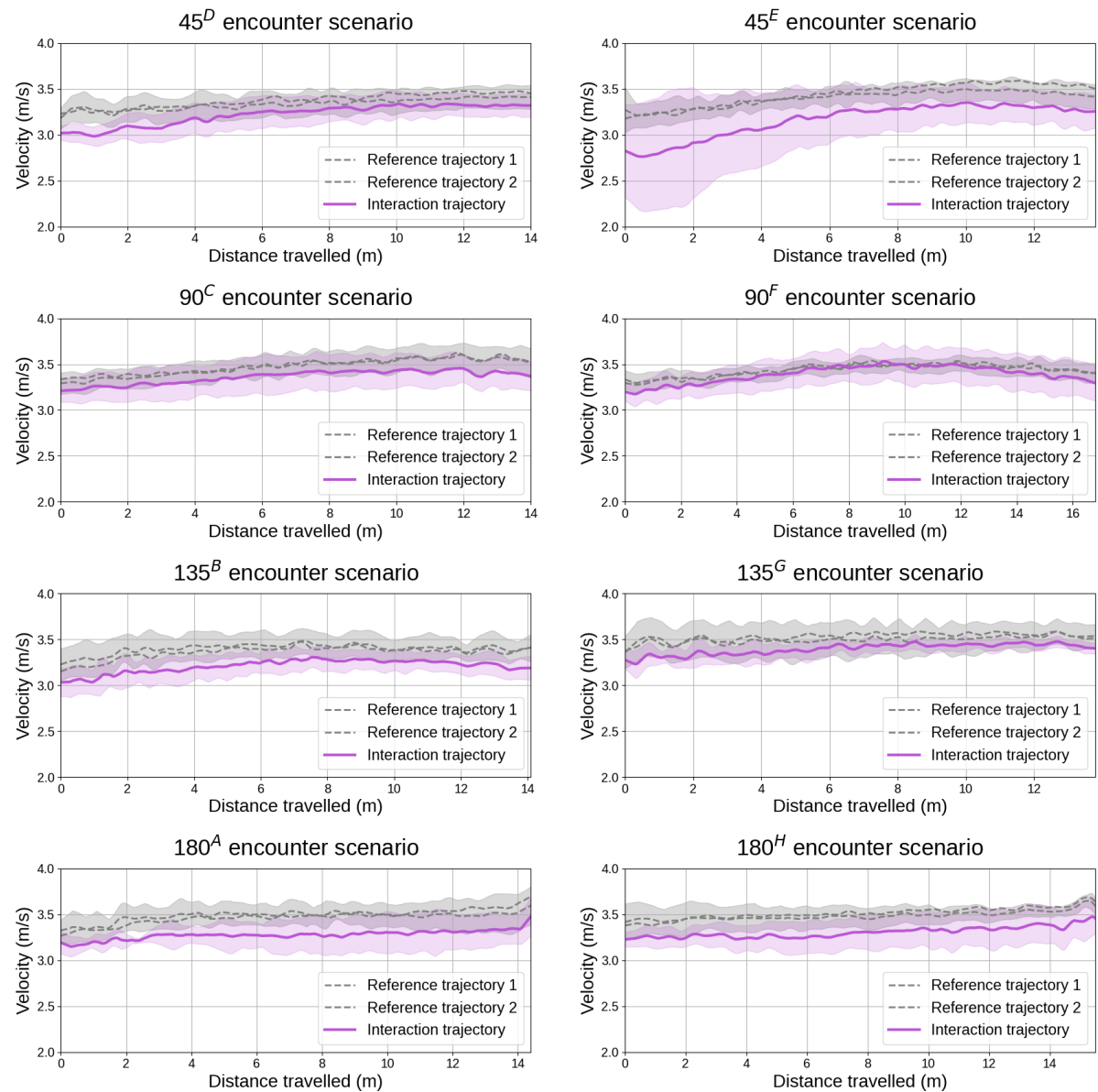
Velocities for All Participants

Figure 6.3: Velocity profiles of all participants, with standard deviations represented by shaded areas. The *grey dashed lines* represent the average velocities for the reference trajectories, while the *purple line* depicts the average velocity profile for the interaction scenario. The rows correspond to different encounter angles: 45°, 90°, 135°, and 180°.

Figure 6.3 illustrates that the 45^E scenario is associated with the greatest variability in velocity, as reflected by the larger shaded region. Additionally, the figure indicates that, excluding the 45^E scenario, average velocities at the point of semi-circle entry consistently exceeded the instructed speed of 2.78 m/s (equivalent to 10 km/h). This observation suggests that participants may have perceived the prescribed speed as overly restrictive or unrepresentative of their natural cycling behavior, instead self-selecting a velocity that better reflected their habitual or comfortable riding pace.

It is observable that the velocity increases at the end of the semi-circle in the 180° encounter scenario. This behavior can be attributed to the uneven surface of the experimental track. In this scenario, the colored cones were positioned just beyond a small depression in the track, resulting in a temporary acceleration.

6.2.2. Velocity selection
Figure 6.4 displays box plots illustrating the comparison of average velocity between the interaction and non-interaction scenarios.
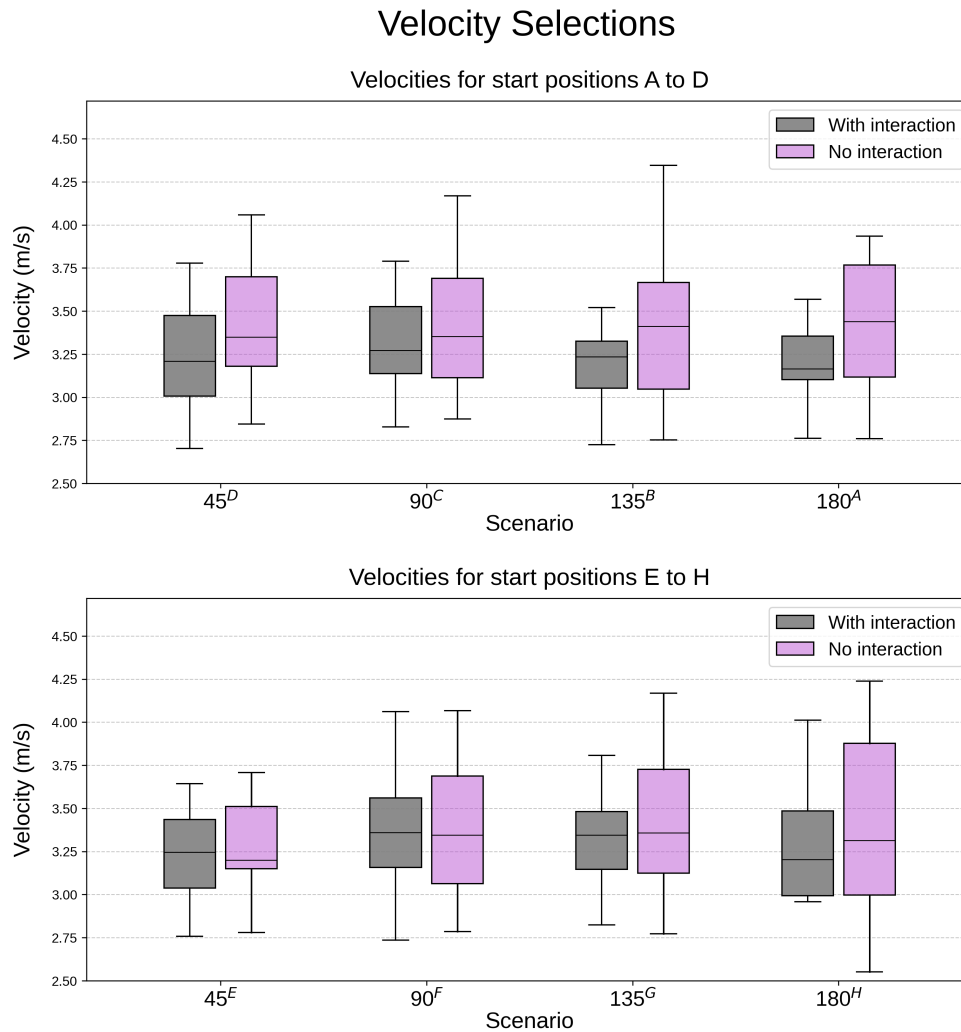
Figure 6.4: Box plots illustrating the average velocities of all participants. The upper plot represents trials in which participants started on the left side of the semi-circle, while the lower plot corresponds to trials where participants began on the right side. *Horizontal black lines* denote medians.

Figure 6.4 demonstrates a high degree of similarity in median cyclist velocities between interaction and non-interaction scenarios. To statistically assess potential velocity differences, three one-way repeated measures ANOVAs were conducted. The results are presented in Table 6.2.

Table 6.2: Summary of results from three separate one-way repeated measures ANOVAs examining average velocity across interaction and non-interaction scenarios.

ANOVA analysis	$F\ (df_1, df_2)$	P-value	η^2
Interaction scenarios	3.21 (7, 133)	**0.0036**	0.15
Non-interaction scenarios	0.39 (7, 133)	0.91	0.020
Interaction vs non-interaction scenarios	5.76 (1, 19)	**0.027**	0.23

Table 6.2 shows that the analyses identified significant differences in average velocities across the eight trials within the interaction scenario. The corresponding η^2 value of 0.15 suggests that only 15% of the variance in average velocity can be attributed to differences between trials. The analysis also revealed a difference between interaction and non-interaction scenarios. However, the associated η^2 value of 0.23 indicates that 23% of the variance in average velocity is explained by scenario type, which does not reflect a large effect size.

To examine pairwise differences among trials within the interaction scenario, 28 post-hoc tests were performed. Despite these tests, no statistically significant differences were found after applying Bonferroni correction. Likewise, pairwise comparisons between interaction and non-interaction scenarios did not reveal any significant differences after Bonferroni correction.

6.2.3. Braking and acceleration patterns
Figure 6.5 displays horizontal acceleration profiles as a function of distance traveled for all participants. The shaded regions, color-coded accordingly, represent one standard deviation, encompassing approximately 68% of the data distribution

Accelerations for All Participants
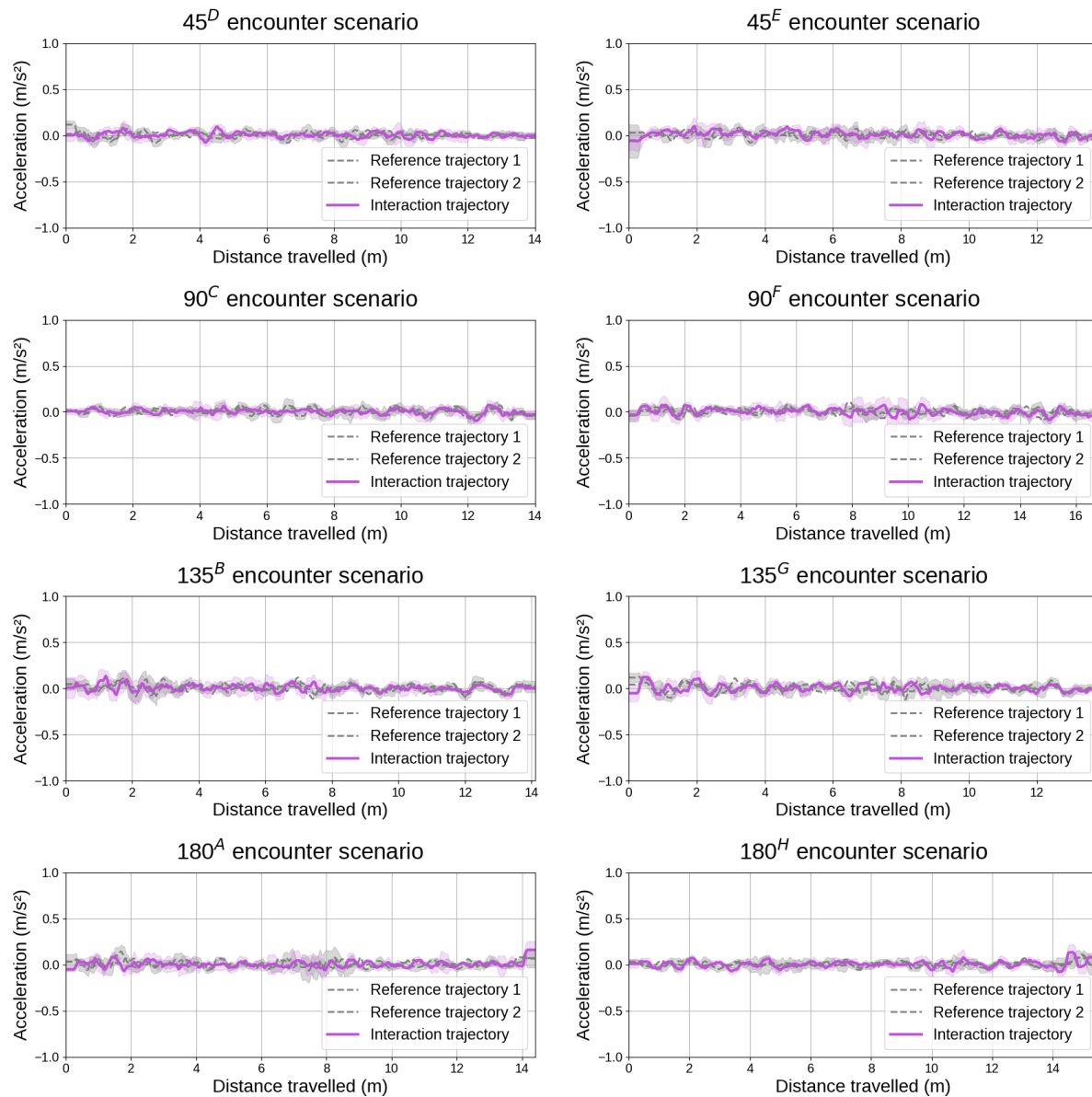
Figure 6.5: Acceleration profiles of all participants, with standard deviations represented by shaded areas. The *grey dashed lines* represent the average accelerations for the reference trajectories, while the *purple line* depicts the average acceleration profile for the interaction scenario. The rows correspond to different encounter angles: 45°, 90°, 135°, and 180°.

Figure 6.5 indicates that no substantial differences in acceleration were observed across scenarios. Acceleration variation appears low, with most values clustered between -0.5 and 0.5 m/s^2. However, the figure presents averaged data, potentially masking subtle braking and acceleration patterns. Minor acceleration fluctuations, likely due to natural pedaling dynamics, are consistent across scenarios and are not expected to affect the overall findings.

Table 6.3 summarizes the statistical tests used to assess differences in average absolute acceleration between interaction and non-interaction scenarios.

Table 6.3: Summary of results from three separate one-way repeated measures ANOVAs examining average absolute acceleration across interaction and non-interaction scenarios.

ANOVA analysis	F (df$_1$, df$_2$)	P-value	η^2
Interaction scenarios	1.24 (7, 133)	0.28	0.062
Non-interaction scenarios	0.69 (7, 133)	0.68	0.035
Interaction vs non-interaction scenarios	0.81 (1, 19)	0.37	0.041

The three separate ANOVAs, as presented in Table 6.3, failed to demonstrate significant differences in average absolute acceleration values across scenarios. It is crucial to acknowledge that this analysis considered participants as a group, not individually. Consequently, the lack of significant findings does not indicate the complete absence of acceleration and braking events.

6.3. Relation path and velocity parameters

This section begins with a systematic analysis of the avoidance strategies employed by cyclist pairs across different scenarios. It then extends the analysis by evaluating correlation coefficients for path adjustments and velocity selections. Finally, the path adjustment ratio and velocity selection ratio are introduced to quantify the extent of these behaviors within each pair.

6.3.1. Avoidance strategies

The contingency table in Figure 6.6 visualizes the distribution of avoidance strategies employed by cyclist pairs, specifically differentiating between path adjustments and changes in selected velocity. The cells of the table contain numerical values indicating the frequency of each strategy

Figure 6.6: Contingency table displaying the frequency of avoidance strategies, categorized by the four different encounter scenarios. For instance, the row labeled 'PA & VS, PA & VS' represents instances where both cyclists in a pair implemented both path adjustments and velocity selection modifications.

Figure 6.6 shows that the 90° scenario is marked by a high frequency of cases where one cyclist adjusts both path and velocity while the other remains passive, suggesting a potential imbalance in collision avoidance responsibility. In contrast, the 180° scenario showed no instances of path adjustment by only one cyclist, unlike the other three encounter scenarios where such cases were present. Additionally, one instance of a passage, defined as neither cyclist making adjustments, was observed. This observation can be attributed to the DTA of approximately four seconds, which eliminated the necessity for the cyclist to make path adjustments.

The Chi-Square test of independence demonstrated a statistically significant association between encounter scenarios and the collision avoidance strategies employed ($\chi^2(21) = 33.97$, $p = 0.037$). Pairwise Chi-Square tests were conducted to identify specific scenario differences in collision avoidance strategies. However, none remained significant after Bonferroni correction.

6.3.2. Correlation coefficient

Table 6.4 presents Pearson correlation coefficients for path adjustments and velocity selections, as well as the correlation between path adjustments and modifications in selected velocity.

Table 6.4: Pearson correlation coefficients and corresponding p-values for path adjustments, velocity selections, and the relationship between path adjustments and velocity selections.

	Path adjustment	Velocity selection	Path and velocity adjustment
Pearson	-0.47	-0.29	0.030
P-value	**9.21e-6**	**0.0097**	0.77

Table 6.4 reports a moderate but statistically significant negative linear relationship of -0.47 for path adjustments. This indicates that when one cyclist adjusts their path to the right, the interacting cyclist tends to adjust their path to the left. For velocity selections, a negative correlation of -0.29 was observed, indicating a weak inverse linear relationship between the velocity choices of two interacting cyclists. This suggests that one cyclist selects a velocity higher than that of their first reference trajectory, while the other chooses a lower velocity in comparison. Additionally, no statistically significant linear relationship was identified between path adjustments and velocity selections, highlighting the complexity and variability of cyclist interaction dynamics.

6.3.3. Path adjustment and velocity selection ratios

As previously discussed, the Pearson correlation coefficient does not capture the magnitude of these adjustments. To address this limitation, path adjustment ratios and velocity selection ratios were computed for each cyclist pair across different encounter scenarios. The results are presented in Table 6.5.

Table 6.5: Path adjustment and velocity selection ratios between two cyclists across different encounter scenarios. The ratios represent the relative magnitude of adjustments made by both cyclists.

	45°	90°	135°	180°
Path adjustment ratio	1 : 3.9	1 : 4.2	1 : 2.6	1 : 3.5
Velocity selection ratio	1 : 14.3	1 : 10.0	1 : 11.9	1 : 6.7

Across all encounter scenarios, the path adjustment ratios indicate a consistent pattern in which one cyclist exhibits greater path adjustments than their counterpart. The most pronounced imbalance occurs in the 90° scenario, where, on average, one cyclist adjusts their path four times more than the other. In contrast, the smallest path adjustment ratio is observed in the 135° scenario. A one-way repeated measures ANOVA, $F(3, 57) = 0.67$, $p = 0.57$, revealed no significant effect of encounter scenario on path adjustment ratios.

Velocity selection ratios indicate an even greater disparity between interacting cyclists, with most scenarios exhibiting highly imbalanced ratios. This suggests that a single cyclist predominantly assumes responsibility for velocity adjustments during these encounters. The one-way repeated measures ANOVA, $F(3, 57) = 0.44$, $p = 0.73$, revealed no significant effect of encounter scenario on velocity selection ratios.

It is noteworthy to mention that the velocity selection ratios may be misleading. Upon closer examination of the data, it becomes evident that the absolute velocity differences are generally small, leading to disproportionately large ratios. For example, if one cyclist exhibits a velocity difference of 0.01 m/s while the other shows a difference of 0.1 m/s, normalization yields a velocity selection ratio of $1 : 10$. In absolute terms, the actual velocity difference between the cyclists is only 0.09 m/s, a relatively minor change that is likely imperceptible to human observers. Therefore, while the ratio suggests a notable disparity in velocity selection, the practical impact of these differences may be minimal.

6.4. Comfort levels

This study examined the relationship between participants' perceived safety and difficulty levels across different encounter scenarios. Table 6.6 presents a summary of the data, where a rating of 1 indicates the lowest perceived safety or the highest perceived difficulty, and a rating of 5 indicates the highest perceived safety or the greatest ease.

Table 6.6: Perceived safety and difficulty levels across the eight different trials. The table presents mean scores for safety perception and difficulty perception.

Scenario	Safety perception	Difficulty perception
45^D	4.30	4.80
45^E	4.15	4.20
90^C	4.60	4.50
90^F	4.45	4.50
135^B	4.55	4.60
135^G	4.50	4.60
180^A	4.55	4.60
180^H	4.55	4.70

Table 6.6 indicates that the 45^E scenario was associated with the lowest perceived safety and the highest perceived difficulty. A one-way repeated measures ANOVA, $F(7, 133) = 1.31$, $p = 0.25$, revealed no significant differences in perceived safety across the various encounter scenarios.

In contrast, a separate one-way repeated measures ANOVA, $F(7, 133) = 133$, $p = 0.0058$, identified a significant effect of scenario on perceived difficulty. However, post-hoc Wilcoxon signed-rank tests did not reveal any statistically significant pairwise differences between specific trials.

7

Statistical Modeling Outcomes

This chapter presents the results of the statistical modeling introduced in Chapter 5, with a focus on understanding cyclist behavior, particularly in relation to yielding decisions. The chapter begins with an overview of the model selection process, followed by a detailed presentation of the modeling results, highlighting key determinants such as DTA, initial velocity differences, approach direction, and cyclist gender. The chapter concludes with a comprehensive evaluation of the model's predictive performance.

7.1. Model selection

As outlined in Chapter 5, the initial step in statistical modeling involves selecting an appropriate model. The model includes five independent variables, as previously presented in Table 5.1, to predict the probability of yielding for each of the 20 participants across a total of 160 trials. In logistic regression analysis, a minimum of ten events per variable is a commonly recommended criterion for sample size considerations (Smeden et al., 2016). Data analysis revealed that in 13 instances, participants ceased pedaling upon entering the semi-circle. With 11 instances of yielding when pedaling ceased and only 2 instances of non-yielding behavior, the scarcity of non-yielding cases poses significant statistical limitations (Ogundimu et al., 2016). Consequently, due to insufficient data, the cadence predictor is not included in the model.

The interaction term between approach direction and encounter angle was also limited by insufficient event counts, failing to meet the minimum of ten events per variable. Specifically, for right-approaching cyclists, yielding occurred in fewer than ten instances across all encounter scenarios, impacting statistical power and potentially leading to random significant results. Therefore, this interaction term was not included in the model.

To address potential participant-level variability, both single-level and multi-level logistic regression models were implemented. The multi-level logistic regression model yielded an ICC of 0.058, indicating that only 5.8% of the variation in the likelihood of yielding can be attributed to differences between participants. Additionally, the LTR was conducted to compare the fit of the single-level logistic regression model and the multi-level logistic regression model. The LRT yielded a test statistic of 1.16, suggesting an improvement in model fit with the inclusion of random effects. However, the associated p-value of 0.28, which exceeds the standard significance threshold of 0.05, indicates that the inclusion of random effects in the multi-level logistic regression model does not significantly enhance the model's fit.

As previously discussed, evaluating the AIC and BIC alongside the LRT offers a more comprehensive assessment of model performance. Table 7.1 presents a comparison of the AIC and BIC values for the single-level and multi-level logistic regression models.

Table 7.1: Comparison of AIC and BIC values for single-level and multi-level logistic regression models to evaluate model fit and complexity.

	AIC	BIC
Single-level logistic regression model	175.48	190.83
Multi-level logistic regression model	176.33	194.74

Table 7.1 demonstrates that the single-level logistic regression model has both lower AIC and BIC values compared to the multi-level logistic regression model. The higher AIC and BIC values for the multi-level model suggest that the inclusion of random effects does not sufficiently improve model fit to justify the added complexity. These findings are consistent with the results of the LRT, which indicated that the random effects were not statistically significant. Given the low ICC, the higher AIC and BIC values, and the results of the LRT, the single-level logistic regression model is selected for this analysis as it achieves a more optimal balance between model fit and simplicity.

While statistical metrics such as AIC, BIC, and LRT are invaluable tools for model selection, practical considerations, including predictive accuracy and generalizability, must also be taken into account to determine the most suitable analytical approach. Accordingly, in addition to the single-level logistic regression model, the multi-level logistic regression model was implemented to further investigate potential heterogeneity in yielding behavior. These models and their results are discussed in detail in Section 7.4 .

7.2. Model collinearity

The VIF values for all predictors are explored and summarized in Table 7.2.

Table 7.2: VIF values for the independent factors, along with their interpretation in terms of multicollinearity risk.

Independent factor	VIF	Interpretation
DTA	1.77	No collinearity
Gender	1.03	No collinearity
Initial velocity difference	1.33	No collinearity
Approach direction	1.86	No collinearity

Table 7.2 shows that all VIF values are below 1.86, indicating the absence of significant collinearity issues among the predictors, as VIF values exceeding 5 are typically considered indicative of multicollinearity concerns. Consequently, model coefficients can be considered robust and reliable.

7.3. Model coefficients

Figure 7.1 presents the estimated coefficients for the independent variables in the single-level logistic regression model. These coefficients correspond to the β_k values as defined in Equation 5.1. Predictors whose confidence intervals cross the null-effect line are considered not statistically significant, as their effects cannot be reliably distinguished from zero. Conversely, predictors with confidence intervals that do not overlap the null-effect line are statistically significant, indicating a meaningful effect on the outcome.
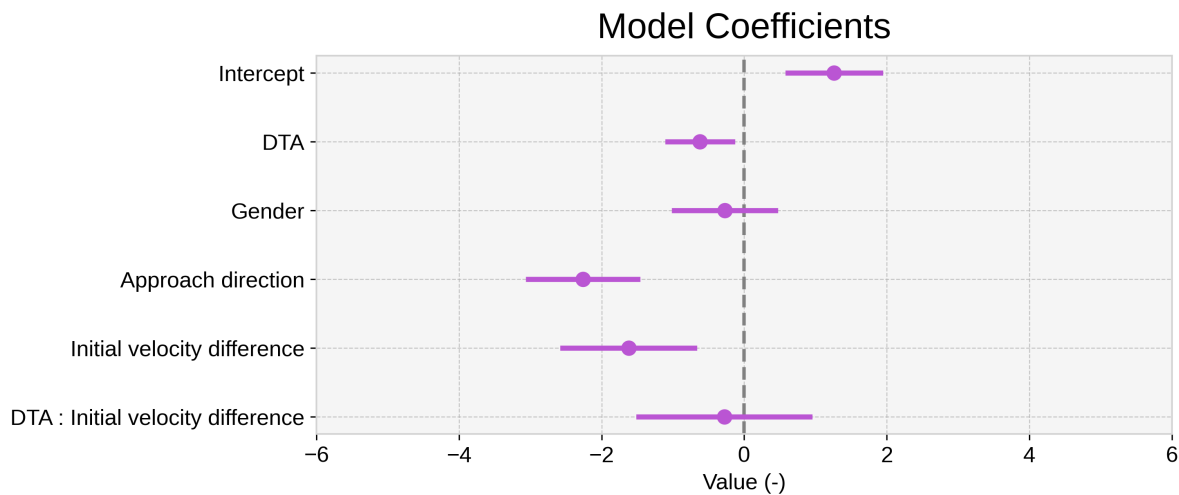
Figure 7.1: Forest plot of the independent variables included in the single-level logistic regression model. The *purple bars* represent the 95% confidence intervals, and the *dots* indicate the mean estimates. The *grey dashed line* represents the null effect.

As depicted in Figure 7.1, the coefficients for DTA, approach direction, and initial velocity difference are statistically significant, as their confidence intervals do not overlap with the null-effect line.

In addition to presenting the model coefficients, it is beneficial to include the multiplicative change in odds for the predictor variables. This approach converts the log-odds coefficients into a more intuitive scale through the exponentiation of the β_k values. This provides a clearer understanding of the effect size. A detailed overview of the multiplicative changes in odds is provided in Table 7.3.

Table 7.3: Multiplicative change in odds for predictor variables, along with confidence intervals and corresponding p-values, derived from the single-level logistic regression analysis.

Variable	Multiplicative change in odds	95%	5%	P-value
Intercept	3.54	7.05	1.78	**0.00032**
DTA	0.54	0.32	0.89	**0.016**
Gender	0.76	0.36	1.62	0.48
Approach direction	0.10	0.046	0.24	**6.51e-8**
Initial velocity difference	0.20	0.070	0.52	**0.0011**
DTA : Initial velocity difference	0.22	2.61	2.08	0.66

Table 7.3 offers a detailed interpretation of the effects of predictor variables on the likelihood of yielding behavior. The model intercept represents the baseline log-odds of yielding, corresponding to the probability of yielding when all predictor variables are set to their reference levels. For the binary variables, specifically gender and approach direction, the baseline corresponds to being female and approaching from the right. Continuous variables, such as DTA and initial velocity difference, are assumed to be zero at baseline. Under these baseline conditions, the odds of yielding are estimated to be 3.54 times greater than the odds of not yielding. The p-value of 0.00032 indicates that this estimate is statistically significant. The predictor variables in the model will further influence the overall probability of yielding.

The DTA is associated with a statistically significant multiplicative change in odds of 0.54, indicating a 46% reduction in the odds of yielding for each one-unit increase in DTA. This result implies that cyclists who enter the semi-circle earlier relative to their interacting opponent exhibit a lower likelihood

of yielding.

Similarly, approach direction is associated with a pronounced multiplicative change in odds of 0.10, reflecting a 90% decrease in the odds of yielding for cyclists approaching from the right. Initial velocity difference also exerts a significant influence, with a multiplicative change in odds of 0.20, indicating that higher initial velocities relative to the interacting opponent are associated with a lower likelihood of yielding.

In contrast, the gender variable exhibits a p-value exceeding the conventional threshold of 0.05, indicating that its effect on the odds of yielding is not statistically significant in this analysis. Similarly, the interaction term between DTA and initial velocity difference does not significantly influence yielding behavior. This finding suggests that the combined effect of these two variables is insufficient to provide meaningful insights beyond their individual contributions.

Although the interaction term between approach direction and encounter angle could not be included in the model, a quantitative assessment of their combined effect on yielding behavior was conducted. Figure 7.2 shows yielding counts across encounter scenarios, categorized by approach direction, allowing for differentiation between the effects of encounter angle and approach direction.
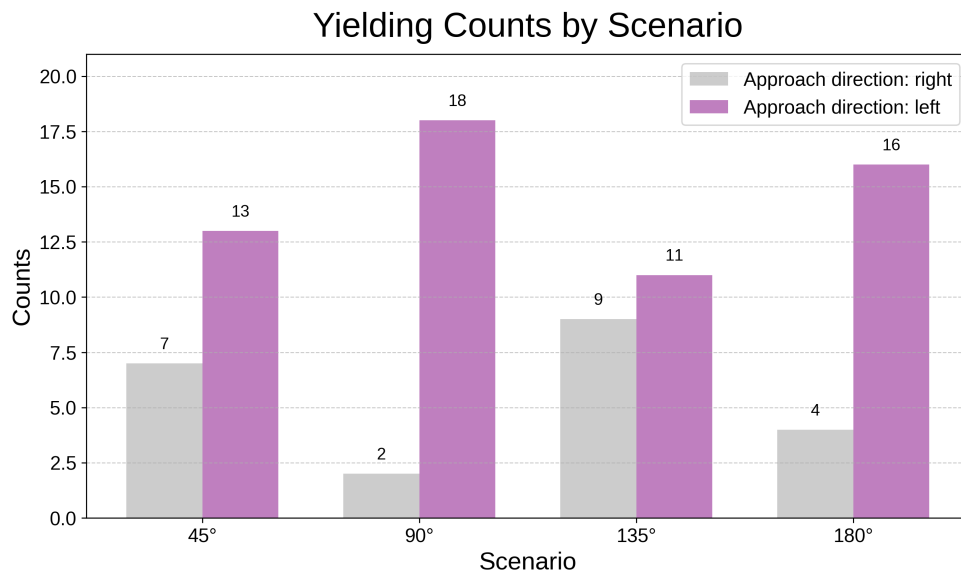

Figure 7.2: Yielding counts for the 45°, 90°, 135°, and 180° scenarios, categorized by whether the yielding cyclist approaches from the left or right side of the semi-circle.

Figure 7.2 suggests that approach direction may influence different encounter scenarios. To statistically validate this, a Chi-Square test was performed. However, no statistically significant association was found between encounter scenario and approach direction ($\chi^2(3)$ = 7.3, p = 0.064).

7.4. Model performance

Although the single-level logistic regression model was deemed most appropriate for this analysis, a multi-level logistic regression model was also implemented to assess model performance and enable a comprehensive comparison.

Table 7.4 presents a detailed comparison of the predictive accuracy of the single-level logistic regression model, the multi-level logistic regression model, and the dummy classifier. As described in Chapter 5, LOOCV was utilized to assess the models' predictive performance.

Table 7.4: Comparison of the predictive accuracy of the single-level logistic regression model, the multi-level logistic regression model, and the dummy classifier.

Statistical model	Predictive accuracy (%)
Single-level logistic regression	76.57
Multi-level logistic regression	77.51
Dummy classifier	48.01

Table 7.4 shows that the multilevel logistic regression model achieved a marginally higher accuracy compared to the single-level logistic regression model. Additionally, the table shows that both models outperform the dummy classifier. The superior performance of the logistic regression models indicate their ability to capture underlying data patterns rather than relying on random guesses or simple heuristics.

It is worth noting that the predictors deemed significant in the single-level logistic regression model remained significant in the multi-level logistic regression model.

8
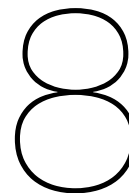
Discussion

This chapter provides a critical evaluation of the study's findings and limitations while also proposing directions for future research. It begins with an in-depth assessment of the kinematic data analysis, followed by a thorough examination of the statistical modeling approach.

8.1. Kinematic data analysis

The findings of this study suggest that cyclists primarily relied on trajectory adjustments rather than speed modulation when interacting with another cyclist. This preference for path adjustment can be attributed to several factors. Firstly, trajectory changes are generally more energy-efficient, as frequent acceleration and deceleration involve greater metabolic cost than maintaining a consistent speed (Vansteenkiste et al., 2017). Secondly, adjusting one's path allows for smoother and more stable control of the bicycle, which is particularly advantageous given the potential balance disturbances associated with abrupt speed changes or riding at low velocities. Furthermore, lateral movements serve as salient social cues, allowing interacting cyclists to more effectively interpret each other's intentions. In contrast, subtle velocity changes are less visually apparent, making them a less reliable medium for non-verbal coordination in dynamic encounters.

Observational data further revealed that participants frequently looked at each other before entering the semi-circle, indicating that anticipation and real-time assessment of the other cyclist's behavior play a critical role in shaping avoidance strategies. The overall Chi-Square test supported the idea that avoidance strategies depend on the specific encounter scenario. However, the absence of significant differences in pairwise comparisons suggests a need for larger datasets to robustly detect scenario-specific effects. This raises a discussion regarding the threshold-based classification employed in this study. While this binary approach, which classified path adjustments and velocity modifications based on predefined thresholds, provides analytical clarity, it introduces limitations. The use of hard thresholds may oversimplify the continuous and dynamic nature of human movement, potentially overlooking subtle but meaningful variations. When applying a higher threshold, as shown in Appendix G.2, the outcomes change and a greater number of interactions are classified as passages. Interestingly, all identified passages again occur within the 135° encounter scenario and are, once more, associated with larger DTA values. A possible explanation for why this occurs exclusively in the 135° scenario is that it was the first scenario encountered by participants. Some participants may have been uncertain about the situation and thus delayed mounting their bicycles, resulting in larger DTA values and the absence of real interactions. However, this explanation remains speculative. These findings clearly demonstrate that threshold selection influences both the distribution of outcomes and the interpretation of strategy patterns across scenarios. Employing alternative methods, including continuous variable analysis, or clustering techniques, could yield more detailed and informative results.

It is also important to note that cyclist interactions are inherently dynamic. Unlike studies that use a robotic or dummy cyclist behaving identically across trials, this study examined the interaction between two independently navigating individuals. As a result, behavioral variability is expected. A more

controlled setup might produce more consistent avoidance patterns, but it would also limit the ecological validity of the findings. Therefore, understanding the decision-making processes in naturalistic cyclist interactions requires a more nuanced approach that accounts for mutual adaptation and unpredictability.

While acknowledging the natural variability inherent in human movement, consistent patterns emerged from the data. These patterns are visualized in Figure 6.1 but are more distinctly evident in the raw trajectory data provided in Appendix G. In the 45° and 90° scenarios, yielding cyclists frequently cut inward toward the center, taking a more direct route through the intersection, while non-yielding cyclists adjusted their trajectories outward. In contrast, this pattern is reversed in the 135° and 180° scenarios, where the non-yielding cyclists are more likely to take the inward, direct route, and the yielding cyclists veer outward. This shift in strategy can be explained by the spatial dynamics of each scenario and the role of the yielding cyclist, which in this study is defined as the cyclist who crosses the intersection last, after the resolution of the interaction. As a result, the yielding cyclist always passes behind the non-yielding cyclist's path. In the 45° and 90° encounters, this spatial relationship allows the yielding cyclist to efficiently cut inward behind the other cyclist without creating conflict. However, in the 135° and 180° scenarios, which involve more frontal approaches, an inward path by the yielding cyclist would lead to a potential head-on interaction. In these situations, the yielding cyclist adapts by veering outward, thereby creating space for the non-yielding cyclist to take the more direct path through the center of the interaction area. This behavior reflects a consistent spatial strategy in which the cyclist who crosses first maintains a more efficient, straight-line trajectory, while the yielding cyclist adjusts their path to accommodate the other. This directional asymmetry helps explain the unequal path adjustment ratios observed in this study. Furthermore, the pattern reinforces the idea that collision avoidance strategies are shaped not only by social roles and scenario geometry but also by the temporal sequencing of the interaction. This complementary movement strategy is further supported by the negative Pearson correlation coefficient, suggesting a systematic, mutual adjustment aimed at maintaining a comfortable interpersonal distance.

The 90° scenario offered particularly compelling insights into social expectations and cultural norms. Here, 18 out of 20 participants approaching from the left yielded, suggesting a shared understanding of right-of-way dynamics. This behavior aligns with Dutch traffic regulations, where cyclists approaching from the right are generally granted priority. Because the 90° scenario closely resembles a standard intersection, participants appeared to apply real-world traffic norms to this experimental context. This highlights how prior experience, traffic culture, and environmental familiarity can influence decision-making in dynamic interactions.

Interestingly, the study observed an absence of hard evasive maneuvers, even in more acute-angle scenarios such as the 45° scenario. Lee et al. (2020) demonstrated that cyclists generally prefer to adjust their path when feasible, resorting to braking only when no alternative is available. Highly evasive maneuvers are generally observed in situations where cyclists have limited reaction time before reaching a conflict zone. One way to simulate such urgency would have been to introduce a visual shield in the experiment, restricting participant's ability to see each other until they entered the semi-circle. This reduced visibility would have shortened the available reaction time, likely resulting in more abrupt and decisive avoidance maneuvers. The absence of such behaviors may also be attributed to the fact that the instructed speed of 10 km/h, which cyclists were asked to maintain until reaching the semi-circle, may have been too low to elicit these avoidance patterns. Moreover, in more acute-angle encounters, such as the 45° scenario, participants were observed to select velocities exceeding 10 km/h. This is particularly noteworthy given the expectation that this scenario would elicit the highest level of discomfort, an expectation that was confirmed by participant responses in the questionnaire. Consequently, it was anticipated that cyclists would exhibit greater caution by reducing their speed. However, the findings indicate that, even under conditions presumed to be the most challenging, cyclists did not perceive a need to decrease their velocity. This may also be the reason why there were no differences found between interaction and non-interaction scenarios within the velocity selection analysis.

As previously mentioned, since each participant had two reference trajectories, all statistical analyses presented in the main body of the thesis were conducted twice. The corresponding results based

on the second reference trajectory are included in the Appendix. Notably, these additional analyses did not reveal any significant differences compared to those reported in the main text, suggesting that participant behavior in terms of trajectory and velocity in non-interaction scenarios is largely consistent across both reference trajectories.

In several cases, the primary statistical tests, whether ANOVA or Chi-square, indicated a significant overall effect, whereas subsequent post hoc analyses did not identify any significant pairwise differences. This discrepancy may be attributed to relatively small and distributed effects that contribute to overall variance but are not individually strong enough to reach significance following Bonferroni correction. This outcome likely reflects limited statistical power, influenced by both the conservative nature of the correction and the sample size. Future research with larger datasets or the application of less conservative post-hoc procedures may provide greater clarity regarding these effects.

8.2. Statistical modeling

The primary objective of the statistical model in this study was to identify the characteristics that underlie yielding behavior. In this study, yielding behavior was represented as a binary variable. Haperen et al. (2018) distinguished between four types of yielding: taking, getting, forcing, and receiving. Had this approach been adopted, yielding would have been categorized as a categorical variable rather than a binary one. However, the dataset's size limited the feasibility of this approach, potentially reducing statistical power due to small category sizes and potential imbalances. To mitigate these issues and maximize statistical power, a binary definition of yielding was employed.

The single-level logistic regression model identified three significant predictors of yielding behavior: approach direction, DTA, and initial velocity difference. Approach direction exhibited a strong effect, with a 90% decrease in the odds of yielding for cyclists approaching from the right. This dominant influence likely reflects cultural yielding norms. However, the influence of approach direction warrants further discussion, as it may vary based on participant demographics. In the Netherlands, road users approaching from the right have the right of way. In other countries, such as the United Kingdom, the rule is reversed, granting priority to those approaching from the left. In this study, most participants grew up in the Netherlands, which may have influenced their behavior. This highlights the need for future research to explore whether the impact of approach direction varies for individuals from different countries with differing traffic regulations.

Silvano et al. (2016) argued that the relationship between DTA and yielding probability aligns with the expectation that the road user arriving first at an intersection is more likely to proceed first. This finding aligns with the results of this study. Cyclists with a negative DTA, indicating a later arrival, are more likely to yield. Furthermore, Mohammadi et al. (2023) noted that cyclists rely on physical effort to propel their bikes and tend to preserve their momentum. Consequently, individuals traveling at higher velocities are less likely to yield, making a lower yielding probability expected among faster cyclists. The observation that cyclists entering the semi-circle at lower velocities relative to their opponent are less likely to yield is consistent with the findings reported by Mohammadi et al. (2023).

The results indicated a slight tendency for males to have a lower probability of yielding. French studies suggest a gendered aspect of risk perception, where males tend to overestimate their cycling abilities, while females overestimate their caution (Félonneau et al., 2013). This may explain the observed tendency for lower yielding probability among males. However, gender was not identified as a significant predictor of yielding behavior in this study. Similarly, Mohammadi et al. (2023) also found no significant effect of gender on cyclists' yielding behavior when interacting with a vehicle. This may be because gender is associated with variations in behavior and physiology that influence decision-making, aspects that were not explicitly captured in this study (Stipancic et al., 2016). It is important to mention that due to the study's reliance on female-male interactions, the effect of gender on yielding behavior could not be fully isolated, as a baseline comparison is lacking. To address this, future investigations should incorporate male-male and female-female interaction pairs. This would facilitate a more rigorous analysis of gender's influence, potentially revealing instances where male participants exhibit consistent yielding tendencies across female-male and male-male interactions, thereby demonstrating a lack of

gender-specific variation.

It is important to note that model performance can be enhanced by adopting a shorter prediction horizon. Instead of using the semi-circle entrance as the predictive horizon, a smaller radius to the semi-circle's midpoint could theoretically bring the prediction closer to the intersection point, potentially enhancing behavioral indicator sensitivity. However, model performance was not the main focus of this study.

Beyond examining the underlying characteristics of yielding behavior, models like the one presented in this study could have future applications in AV technology. However, for such models to be effective in this context, they must be developed specifically for interactions between cyclists and AVs rather than cyclist-cyclist interactions. Additionally, predictive algorithms for human behavior in AV systems must achieve significantly higher performance than the model presented in this study, as incorrect predictions in real-world traffic scenarios could be catastrophic and pose serious risks to cyclists.

A promising avenue for future research is the development of a predictive model for cyclists' collision avoidance strategies. However, the dataset used in this study, consisting of 160 observations, lacks the richness necessary for such an endeavor. Predicting cyclist behavior requires distinguishing between path adjustments and velocity modifications while also determining the directionality of these changes, increases the complexity of the modeling process. To achieve this, a categorical classification model would be necessary to categorize cyclists' actions effectively. However, given the dataset's limitations, constructing a reliable predictive model would require either a significantly larger dataset to ensure sufficient variability and model robustness or the implementation of data augmentation techniques. One widely used augmentation approach for handling imbalanced datasets is the Synthetic Minority Oversampling Technique (SMOTE). SMOTE generates synthetic samples by interpolating between existing observations, thereby enhancing data diversity and reducing bias in model training (Matharaarachchi et al., 2024). As observed in Figure 6.6, avoidance strategies are imbalanced within the dataset, indicating that the application of SMOTE could improve model performance and generalizability. Future studies should explore this technique in combination with advanced categorical modeling approaches to better capture cyclist behavior in collision avoidance scenarios. Similarly, SMOTE could be adopted to potentially include model predictors like cadence and the interaction term of approach direction and encounter angle, which were excluded due to insufficient event counts.

9

Conclusion

This study comprises two parts. The first part focused on examining the kinematics of interacting cyclists, specifically addressing the following research question:

How do cyclists adjust their path and speed to avoid collisions in close interactions, and how do these strategies vary across different scenarios?

The findings indicate that cyclists predominantly relied on path adjustments rather than changes in velocity when avoiding collisions. Cyclists generally moved away from one another to preserve space, and there is also evidence suggesting that when one cyclist reduced speed, the other tended to increase theirs. Together, path adjustments and velocity modulation constitute key components of collision avoidance strategies. While the results suggest that these strategies may vary across encounter scenarios, additional data are needed to increase statistical power and draw definitive conclusions, as post-hoc analyses did not reveal statistically significant differences.

The second part of this study aimed to investigate the factors influencing path and speed adjustments, with a particular focus on yielding behavior. This section addresses the following research question:

What interaction characteristics underlie path and speed adjustments involving yielding behavior?

The single-level logistic regression model identified DTA, differences in initial velocity, and approach direction as significant predictors of yielding behavior. Specifically, cyclists who entered the semi-circle later, had lower initial velocities, and approached from the left were more likely to yield than those who did not. To more robustly link yielding behavior to the collision avoidance strategies employed, additional data or the application of data augmentation techniques may be necessary.
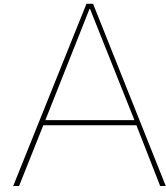
Acknowledgements

Bibliography

Akaike, H. (1974). A new look at the statistical model identification. *IEEE Transactions on Automatic Control*, *19*(6), 716–723. 10.1109/tac.1974.1100705.

Al-Naime, K., Al-Anbuky, A., & Mawston, G. (2020). Human Movement Monitoring and Analysis for Prehabilitation Process Management. *Journal of Sensor and Actuator Networks*, *9*(1), 9. 10.3390/jsan9010009.

Arlot, S., & Celisse, A. (2010). A survey of cross-validation procedures for model selection. *Statistics Surveys*, *4*(none). 10.1214/09-ss054.

Bishop, C. M. (2007). Pattern Recognition and Machine Learning. *Journal of Electronic Imaging*, *16*(4), 049901. 10.1117/1.2819119.

Buehler, R. (2018). Bicycling levels and trends in western europe and the usa. *GeoAgenda*, (1), 10–13.

Chin, H.-C., & Quek, S.-T. (1997). Measurement of traffic conflicts. *Safety Science*, *26*(3), 169–185. 10.1016/s0925-7535(97)00041-6.

Dias, C., Abdullah, M., Hussain, Q., Salehi, A. M., & Nishiuchi, H. (2023). Exploring Microscopic Characteristics of Bicycle Riders' following Behaviors in a Single-File Movement. *Applied Sciences*, *13*(11), 6539. 10.3390/app13116539.

Dormann, C. F., Elith, J., Bacher, S., Buchmann, C., Carl, G., Carré, G., Marquéz, J. R. G., Gruber, B., Lafourcade, B., Leitão, P. J., Münkemüller, T., McClean, C., Osborne, P. E., Reineking, B., Schröder, B., Skidmore, A. K., Zurell, D., & Lautenbach, S. (2012). Collinearity: a review of methods to deal with it and a simulation study evaluating their performance. *Ecography*, *36*(1), 27–46. 10.1111/j.1600-0587.2012.07348.x.

Dunn, O. J. (1961). Multiple comparisons among means. *Journal of the American Statistical Association*, *56*(293), 52. 10.2307/2282330.

Feleke, R., Scholes, S., Wardlaw, M., & Mindell, J. S. (2017). Comparative fatality risk for different travel modes by age, sex, and deprivation. *Journal of Transport Health*, *8*, 307–320. 10.1016/j.jth.2017.08.007.

Félonneau, M.-L., Causse, E., Constant, A., Contrand, B., Messiah, A., & Lagarde, E. (2013). Gender stereotypes and superior conformity of the self in a sample of cyclists. *Accident Analysis Prevention*, *50*, 336–340. 10.1016/j.aap.2012.05.006.

Grigoropoulos, G., Leonhardt, A., Kaths, H., Junghans, M., Baier, M. M., & Busch, F. (2022). Traffic flow at signalized intersections with large volumes of bicycle traffic. *Transportation Research Part A: Policy and Practice*, *155*, 464–483. 10.1016/j.tra.2021.11.021.

Haperen, W., Daniels, S., De Ceunynck, T., Saunier, N., Brijs, T., & Wets, G. (2018). Yielding behavior and traffic conflicts at cyclist crossing facilities on channelized right-turn lanes. *Transportation Research Part F Traffic Psychology and Behaviour*, *55*, 272–281. 10.1016/j.trf.2018.03.012.

Holdcroft, A. (2006). Gender bias in research: how does it affect evidence based medicine? *Journal of the Royal Society of Medicine*, *100*(1), 2–3. 10.1258/jrsm.100.1.2.

Ito, P. (1980, January). *7 Robustness of ANOVA and MANOVA test procedures*. 10.1016/s0169-7161(80)01009-7.

Jong, T. (2009). Cognitive load theory, educational research, and instructional design: some food for thought. *Instructional Science*, *38*(2), 105–134. 10.1007/s11251-009-9110-0.

Kim, M., Kim, E., Oh, J., & Jun, J. (2012). Critical factors associated with bicycle accidents at 4-legged signalized urban intersections in South Korea. *KSCE Journal of Civil Engineering*, *16*(4), 627–632. 10.1007/s12205-012-1055-1.

King, A. P., & Eckersley, R. J. (2019, January). *Inferential Statistics IV: Choosing a Hypothesis Test*. 10.1016/b978-0-08-102939-8.00016-5.

Kumar, A., Kumar, S., Lal, P., Saikia, P., Srivastava, P. K., & Petropoulos, G. P. (2021, January). *Introduction to GPS/GNSS technology*. 10.1016/b978-0-12-818617-6.00001-9.

Lee, O., Rasch, A., Schwab, A. L., & Dozza, M. (2020). Modelling cyclists' comfort zones from obstacle avoidance manoeuvres. *Accident Analysis Prevention*, *144*, 105609. 10.1016/j.aap.2020.105609.

Li, J., Yang, Y., He, H., & Wang, B. (2022). RTK positioning based on the phase-only differential corrections. *Advances in Space Research*, *70*(4), 880–889. 10.1016/j.asr.2022.05.029.

Matharaarachchi, S., Domaratzki, M., & Muthukumarana, S. (2024). Enhancing SMOTE for imbalanced data with abnormal minority instances. *Machine Learning with Applications*, 100597. 10.1016/j.mlwa.2024.100597.

Mohammadi, A., Piccinini, G. B., & Dozza, M. (2023). How do cyclists interact with motorized vehicles at unsignalized intersections? Modeling cyclists' yielding behavior using naturalistic data. *Accident Analysis Prevention*, *190*, 107156. 10.1016/j.aap.2023.107156.

Montgomery, D. C., Peck, E. A., & Vining, G. (2010, October). *Introduction to Linear Regression Analysis*. 10.1201/b10289-6.

Moore, J. K. (2012). *Human control of a bicycle* [Doctoral dissertation, University of California].

Nikitas, A., Tsigdinos, S., Karolemeas, C., Kourmpa, E., & Bakogiannis, E. (2021). Cycling in the Era of COVID-19: Lessons Learnt and Best Practice Policy Recommendations for a More Bike-Centric Future. *Sustainability*, *13*(9), 4620. 10.3390/su13094620.

Ogundimu, E. O., Altman, D. G., & Collins, G. S. (2016). Adequate sample size for developing prediction models is not simply related to events per variable. *Journal of Clinical Epidemiology*, *76*, 175–182. 10.1016/j.jclinepi.2016.02.031.

Ramsey, N. (1983). History of Atomic Clocks. *Journal of Research of the National Bureau of Standards*, *88*(5), 301. 10.6028/jres.088.015.

Safonova, A., Ghazaryan, G., Stiller, S., Main-Knorn, M., Nendel, C., & Ryo, M. (2023). Ten deep learning techniques to address small data problems with remote sensing. *International Journal of Applied Earth Observation and Geoinformation*, *125*, 103569. 10.1016/j.jag.2023.103569.

Schwarz, G. (1978). Estimating the Dimension of a Model. *The Annals of Statistics*, *6*(2). 10.1214/aos/1176344136.

Senter, H. F. (2008). Applied Linear Statistical Models. *Journal of the American Statistical Association*, *103*(482), 880. 10.1198/016214508000000300.

Shapiro, S. S., & Wilk, M. B. (1965). An analysis of variance test for normality (complete samples). *Biometrika*, *52*(3-4), 591–611. 10.1093/biomet/52.3-4.591.

Silvano, A. P., Koutsopoulos, H. N., & Ma, X. (2016). Analysis of vehicle-bicycle interactions at unsignalized crossings: A probabilistic approach and application. *Accident Analysis Prevention*, *97*, 38–48. 10.1016/j.aap.2016.08.016.

Smeden, M., De Groot, J. A. H., Moons, K. G. M., Collins, G. S., Altman, D. G., Eijkemans, M. J. C., & Reitsma, J. B. (2016). No rationale for 1 variable per 10 events criterion for binary logistic regression analysis. *BMC Medical Research Methodology*, *16*(1). 10.1186/s12874-016-0267-3.

Stipancic, J., Zangenehpour, S., Miranda-Moreno, L., Saunier, N., & Granié, M.-A. (2016). Investigating the gender differences on bicycle-vehicle conflicts at urban intersections using an ordered logit methodology. *Accident Analysis Prevention*, *97*, 19–27. 10.1016/j.aap.2016.07.033.

Swift Navigation. (2024). Swift Navigation. https://www.swiftnav.com/

Useche, S., Montoro, L., Tomás, J., & Cendales, B. (2018a). Validation of the cycling behavior questionnaire: A tool for measuring cyclists' road behaviors. *Transportation Research Part F Traffic Psychology and Behaviour*, *58*, 1021–1030. 10.1016/j.trf.2018.08.003.

Useche, S. A., Alonso, F., Montoro, L., & Esteban, C. (2018b). Explaining self-reported traffic crashes of cyclists: An empirical study based on age and road risky behaviors. *Safety Science*, *113*, 105–114. 10.1016/j.ssci.2018.11.021.

Vansteenkiste, P., Zeuwts, L., Van Maarseveen, M., Cardon, G., Savelsbergh, G., & Lenoir, M. (2017). The implications of low quality bicycle paths on the gaze behaviour of young learner cyclists. *Transportation Research Part F Traffic Psychology and Behaviour*, *48*, 52–60. 10.1016/j.trf.2017.04.013.

Vehtari, A., Gelman, A., & Gabry, J. (2016). Practical Bayesian model evaluation using leave-one-out cross-validation and WAIC. *Statistics and Computing*, *27*(5), 1413–1432. 10.1007/s11222-016-9696-4.

Wexler, M. S., & El-Geneidy, A. (2017). Keep 'Em Separated: Desire Lines Analysis of Bidirectional Cycle Tracks in Montreal, Canada. *Transportation Research Record Journal of the Transportation Research Board*, *2662*(1), 102–115. 10.3141/2662-12.

Wilcoxon, F. (1945). Individual Comparisons by Ranking Methods. *Biometrics Bulletin*, *1*(6), 80. 10 . 2307/3001968.

Appendix

A.1. Questionnaires

Figure A.1: Questionnaire on perceived safety and trial difficulty. Participants assessed their perception of safety and the ease of each trial. They were required to complete the corresponding questions after each trial.

Rider Characteristics Questions
Cyclist Interaction Experiment

Please answer the following questions.

What is your current age in years?

_____ years

What is your gender? Choose an option or describe yourself.

Woman   Man   Non-binary   Prefer not to say

How many years of cycling experience do you have?

| Less than 1 year | 1 – 2 years | 2 – 5 years | 5 – 10 years | More than 10 years |

How much time did you regularly spend cycling the past year? Please estimate in hours per week.

_____ hours per week

What type of bicycles did you ride regularly in the past year? Multiple answers are possible.

City bike   Touring bike   Race bike   Mountain bike   Cargo bike

City e-bike   Touring e-bike   Race e-bike   Mountain e-bike   Cargo e-bike

What do you use your bicycle for? Multiple answers are possible.

Commuting   General mobility   Recreation

Competitive sports   Work

Figure A.2: Rider characteristics questionnaire. Participants were required to complete this questionnaire prior to the commencement of the experiment.

Experiment Experience Questions

Cyclist Interaction Experiment

Please answer the following questions.

Did the instrumented bicycle you rode feel different than the bicycles that you are used to?

Yes   No   I don't know

If yes, in what way?

_____

_____

To what extent do these interactions reflect real-world cycling interactions?

Not at all   Slightly   Somewhat   Mostly   Completely

If the interactions did not reflect real-world cycling interaction, please explain why?

_____

_____

_____

Do you feel you interacted with the other cyclist in a way similar to how you would in a real-world setting?

Not at all   Slightly   Somewhat   Mostly   Completely

If the interactions did not feel similar to a real-world setting, please explain why?

_____

_____

_____

Figure A.3: Experiment experience questionnaire. Participants were required to complete this questionnaire upon completion of the experiment.

B
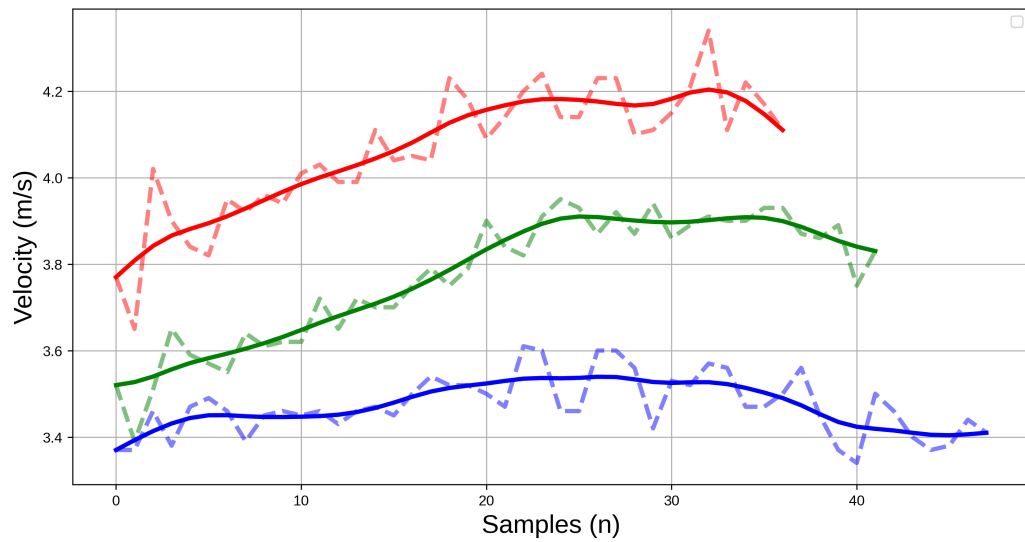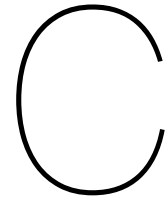
Appendix

B.1. Butterworth filter

Figure B.1: Impact of a second-order low-pass Butterworth filter on raw velocity data, using a cutoff frequency of 2 Hz. *Solid colored lines* represent filtered velocity data, while *striped lines* represent unfiltered velocity. The upper two lines depict velocity in the reference trajectories, and the lowest line shows the interaction trajectory.

C

Appendix

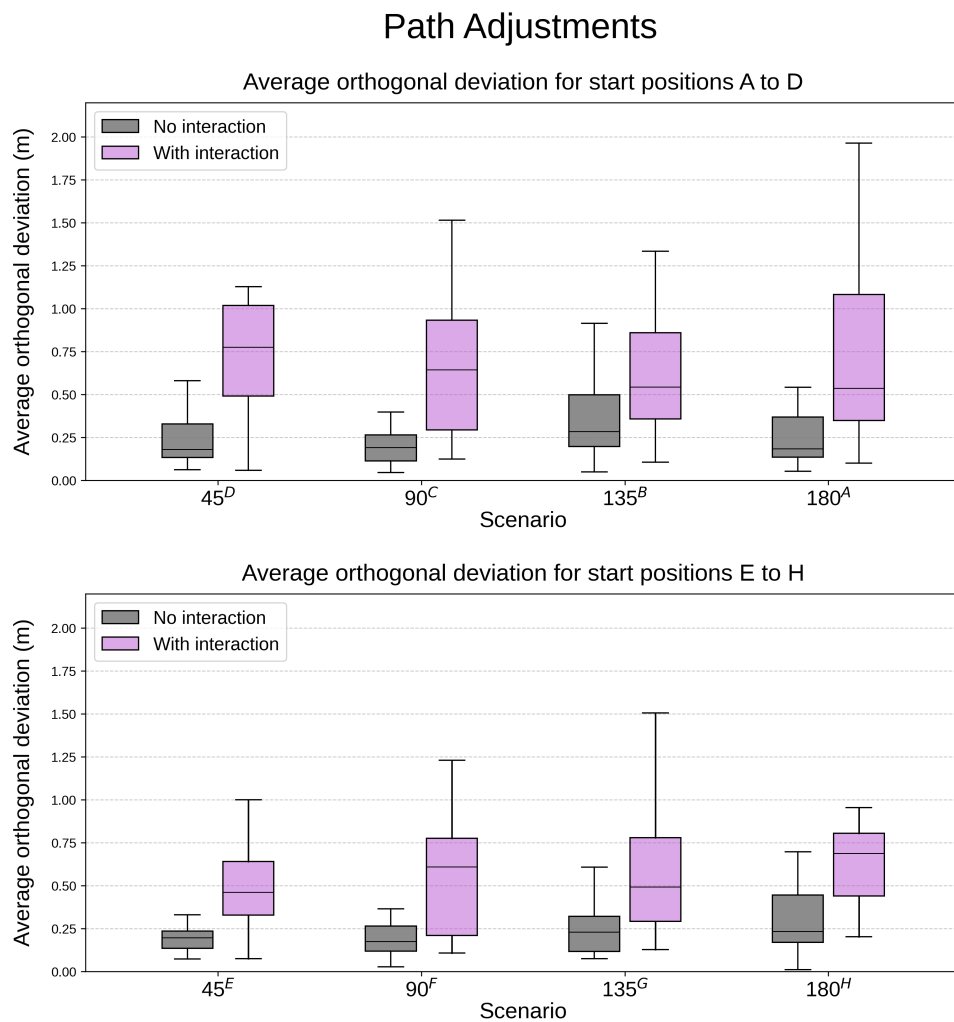## C.1. Path adjustment box plots

Path Adjustments

Figure C.1: Box plots comparing path adjustments in interaction and non-interaction scenarios based on average orthogonal deviation. The upper plot represents trials where participants started on the left side of the semi-circle, while the lower plot represents trials where participants started on the right side. *Horizontal black lines* denote medians.

C.2. ANOVA path adjustment analysis

Table C.1: Summary of results from three separate one-way repeated measures ANOVAs examining average orthogonal deviation across interaction and non-interaction scenarios using the second reference trajectory. Statistically significant p-values are shown in bold.

ANOVA analysis	F (df_1, df_2)	P-value	η^2
Interaction scenarios	1.68 (7, 133)	0.12	0.082
Non-interaction scenarios	0.64 (7, 133)	0.72	0.033
Interaction vs non-interaction scenarios	0.81 (1, 19)	**0.00**	0.75

C.2.1. Post-hoc analysis

Table C.2: Overview of the statistical tests conducted to assess differences in average orthogonal deviation between interaction and non-interaction scenarios. The first column lists the encounter scenarios. The second column specifies the effect size for both analyses, using the first and second reference trajectories, respectively. Negative signs indicate that average orthogonal deviations were lower in non-interaction scenarios compared to interaction scenarios. A significance threshold of $\alpha = 0.00625$ was used, adjusted for multiple comparisons. P-values from pairwise comparisons using both the first and second reference trajectories are reported. Statistically significant p-values are shown in bold.

Scenario	Effect size	P-values
45^D	-0.86, -0.84	**0.0000, 0.0000**
45^E	-0.71, -0.79	**0.0001, 0.0007**
90^C	-0.82, -0.73	**0.0004, 0.0005**
90^F	-0.74, -0.82	**0.0003, 0.0000**
135^B	-0.79, -0.45	**0.0001, 0.0000**
135^G	-0.58, -0.83	0.0083, 0.044
180^A	-0.69, -0.60	**0.0012, 0.0056**
180^H	-0.76, -0.83	**0.0002, 0.0000**

C.3. ANOVA path adjustment ratio

Table C.3: Path adjustment ratios between two cyclists across different encounter scenarios. The ratios represent the relative magnitude of adjustments made by both cyclists.

	45°	90°	135°	180°
Path adjustment ratio	1 : 3.6	1 : 4.2	1 : 3.0	1 : 3.2

Table C.4: Results of a one-way repeated measures ANOVA examining differences in path adjustment ratios across four encounter scenarios. This table presents the analysis based on the second reference trajectory, which was used to compute the average orthogonal deviation for each cyclist pair. The corresponding ANOVA results based on the first reference trajectory are reported in the main text. Both ANOVAs revealed no significant differences in path adjustment ratios across the four encounter scenarios.

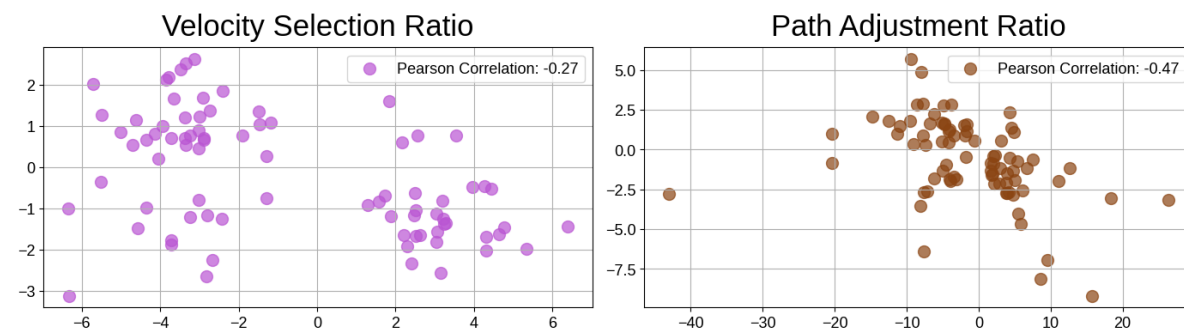| ANOVA analysis	F (df$_1$, df$_2$)	P-value	η^2
Interaction scenarios	0.96 (3, 57)	0.42	0.13

C.4. Correlation coefficients

Figure C.2: Correlations between path adjustments and velocity selections using the first reference trajectory. The left panel illustrates correlations among path adjustments within each cyclist pair. The right panel illustrates correlations among velocity selections within each cyclist pair.

D
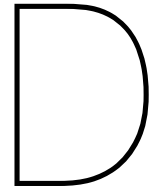
Appendix

D.1. Velocity selection box plots
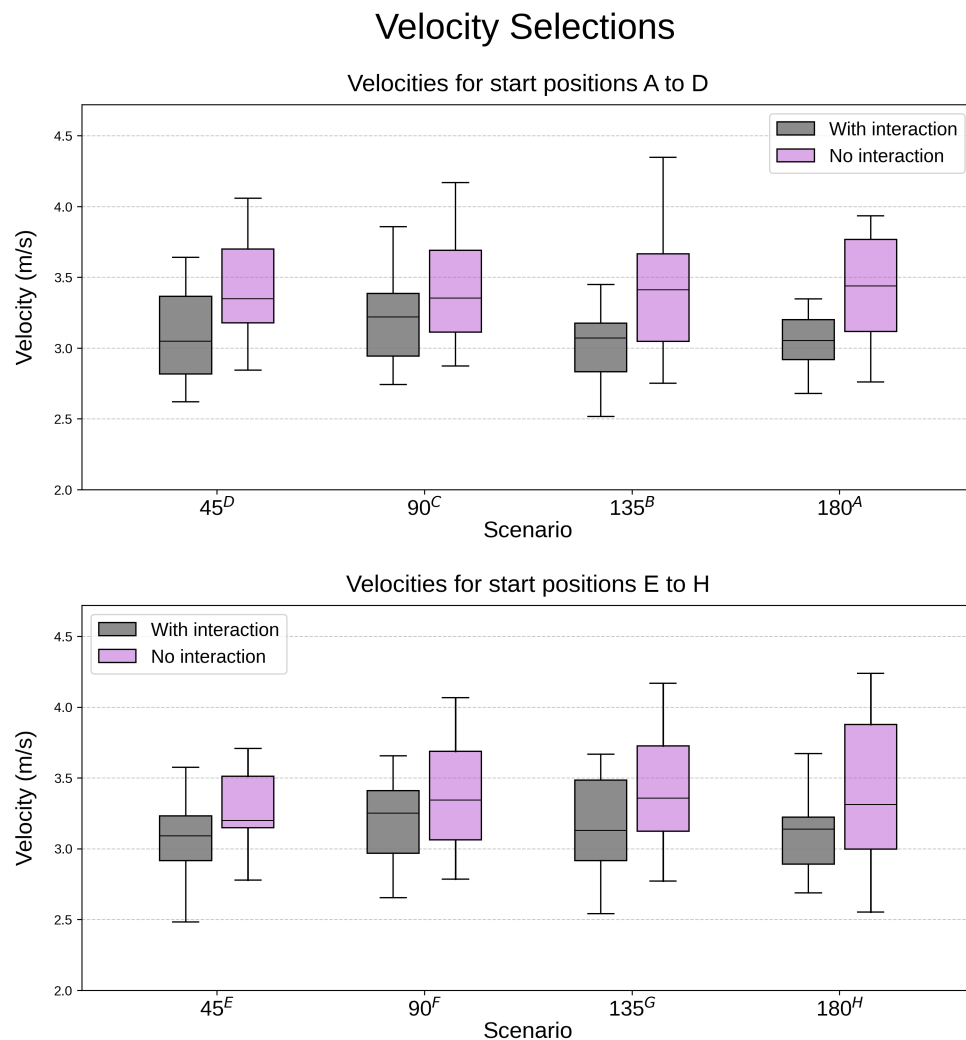
Velocity Selections

Figure D.1: Box plots illustrating the average velocities of all participants. The upper plot represents trials in which participants started on the left side of the semi-circle, while the lower plot corresponds to trials where participants began on the right side. *Horizontal black lines* denote medians.

D.2. ANOVA velocity selection analysis

Table D.1: Summary of results from three separate one-way repeated measures ANOVAs examining average velocity across interaction and non-interaction scenarios using the second reference trajectory. Statistically significant p-values are shown in bold.

ANOVA analysis	F (df_1, df_2)	P-value	η^2
Interaction scenarios	2.09 (7, 133)	**0.049**	0.099
Non-interaction scenarios	0.41 (7, 133)	0.90	0.021
Interaction vs non-interaction scenarios	17.14 (1, 19)	**0.00060**	0.47

D.2.1. Post-hoc analysis

Table D.2: Overview of the statistical tests conducted to assess differences in average velocities between interaction and non-interaction scenarios. The first column lists the encounter scenarios. The second column specifies the effect size for both analyses, using the first and second reference trajectories, respectively. Negative signs indicate that average orthogonal deviations were lower in non-interaction scenarios compared to interaction scenarios. A significance threshold of $\alpha = 0.00625$ was used, adjusted for multiple comparisons. P-values from pairwise comparisons using both the first and second reference trajectories are reported. Statistically significant p-values are shown in bold.

Scenario	Effect size	P-values
45^D	-0.31, -0.42	0.064, 0.18
45^E	-0.50, -0.43	0.053, 0.024
90^C	-0.19, -0.21	0.55, 0.41
90^F	-0.15, -0.075	0.76, 0.55
135^B	-0.49, -0.56	0.011, 0.027
135^G	-0.33, -0.26	0.26, 0.23
180^A	-0.25, -0.35	0.12, 0.28
180^H	-0.30, -0.26	0.28, 0.19

Table D.3: Overview of statistical tests conducted to assess differences in average velocities within interaction scenarios. P-values are reported, using a significance threshold of $\alpha = 0.00178$. Statistically significant p-values are shown in bold.

|	45^D	45^E	90^C	90^F	135^B	135^G	180^A	180^H
45^D	- - -	- - -	- - -	- - -	- - -	- - -	- - -	- - -
45^E	0.96	- - -	- - -	- - -	- - -	- - -	- - -	- - -
90^C	0.019	0.027	- - -	- - -	- - -	- - -	- - -	- - -
90^F	0.014	0.021	0.33	- - -	- - -	- - -	- - -	- - -
135^B	0.18	0.39	0.002	0.001	- - -	- - -	- - -	- - -
135^G	0.14	0.35	0.67	0.47	0.019	- - -	- - -	- - -
180^A	0.96	0.84	0.058	0.0083	0.33	0.23	- - -	- - -
180^H	0.13	0.29	0.52	0.19	0.083	0.78	0.25	- - -

D.3. ANOVA velocity selection ratio

Table D.4: Velocity selection ratios between two cyclists across different encounter scenarios. The ratios represent the relative magnitude of adjustments made by both cyclists.

	45°	90°	135°	180°
Velocity selection ratio	1 : 15.1	1 : 9.8	1 : 12.2	1 : 9.7

Table D.5: Results of a one-way repeated measures ANOVA examining differences in velocity selection ratios across four encounter scenarios. This table presents the analysis based on the second reference trajectory, which was used to compute the difference in average velocity for each cyclist pair. The corresponding ANOVA results based on the first reference trajectory are reported in the main text. Both ANOVAs revealed no significant differences in velocity selection ratios across the four encounter scenarios.

ANOVA analysis	F (df$_1$, df$_2$)	P-value	η^2
Interaction scenarios	0.66 (3, 57)	0.72	0.09

E
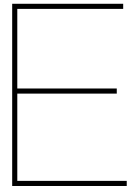
Appendix

E.1. ANOVA absolute acceleration analysis

Table E.1: Summary of results from three separate one-way repeated measures ANOVAs examining average absolute acceleration across interaction and non-interaction scenarios.

ANOVA analysis	F (df_1, df_2)	P-value	η^2
Interaction scenarios	0.69 (7, 133)	0.68	0.035
Non-interaction scenarios	1.97 (7, 133)	0.064	0.094
Interaction vs non-interaction scenarios	0.77 (1, 19)	0.39	0.039

F

Appendix

F.1. Distribution average orthogonal deviations

Histograms of Average Orthogonal Deviation
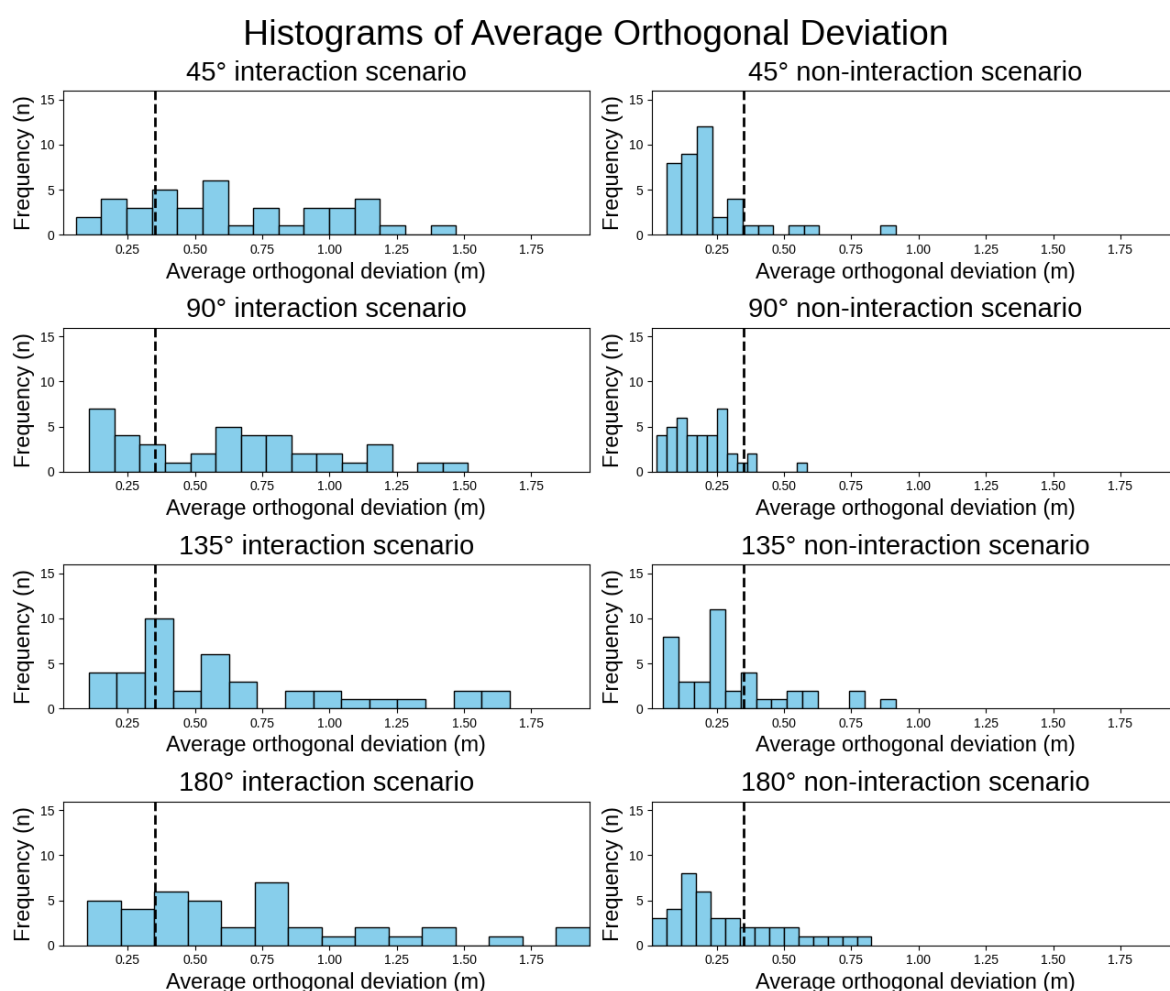
Figure F.1: Histograms representing the distribution of average orthogonal deviation values in various interaction and non-interaction scenarios. The threshold for path adjustment classification is indicated by the *vertical dashed lines*.
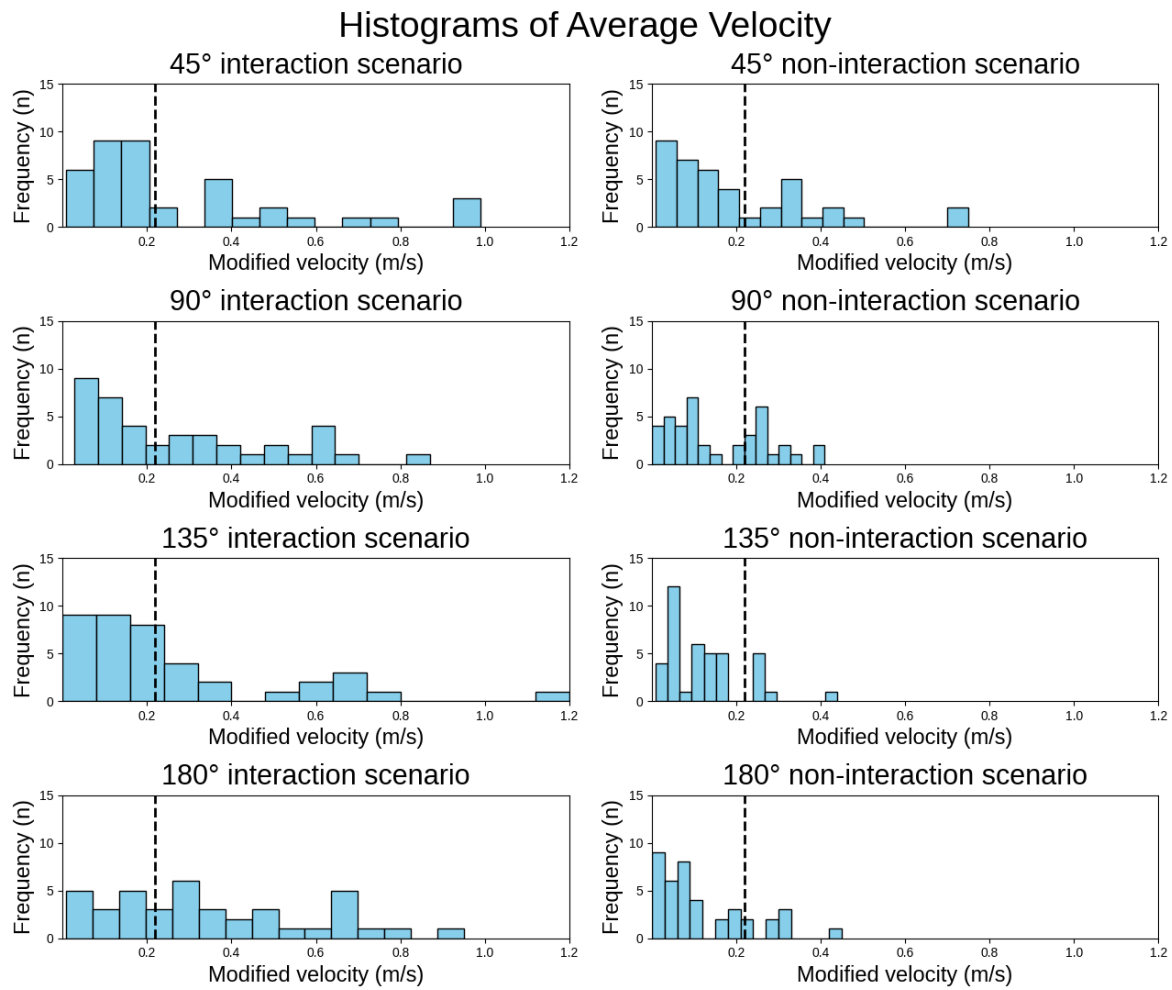
F.2. Distribution average velocity

Figure F.2: Histograms representing the distribution of average velocity values in various interaction and non-interaction scenarios. The threshold for path adjustment classification is indicated by the *vertical dashed lines*.
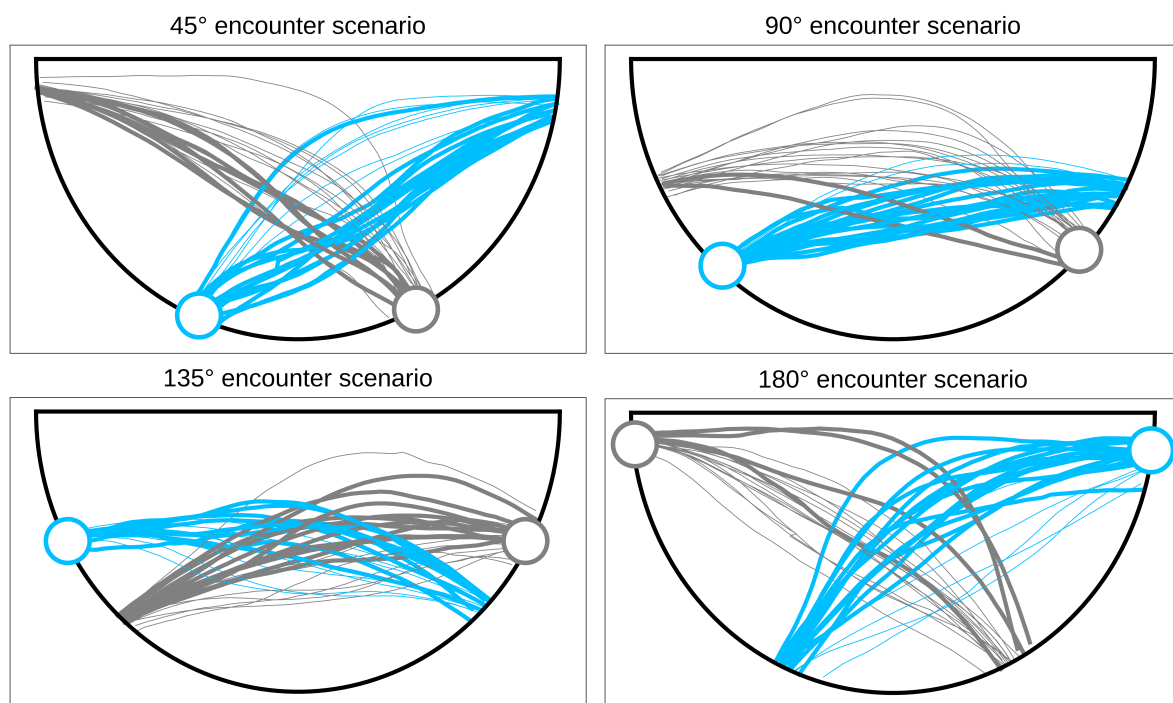
G

Appendix

G.1. Raw trajectory plots

Figure G.1: Raw trajectory plots for each of the four encounter scenarios. Circles indicate starting positions. *Thick lines* represent yielding cyclists, and *thin lines* represent non-yielding cyclists.

G.2. Contingency table with increased thresholds

Figure G.2: Contingency table presenting the distribution of avoidance strategies across four encounter scenarios. A threshold of $\Delta \overline{v}_{ref} + 2\sigma_{\Delta v_{ref}}$ for velocity and $\Delta \overline{P}_{ref} + 2\sigma_{\Delta P_{ref}}$ for path adjustments was used. Under these conditions, four passages were detected, all occurring within the 135° encounter scenario. This highlights the impact of the applied thresholding method. A Chi-square test confirmed that avoidance strategies and encounter scenarios were significantly dependent, $\chi^2(27) = 43.15$, $p = 0.025$. Post hoc comparisons revealed no significant differences across the encounter scenarios.
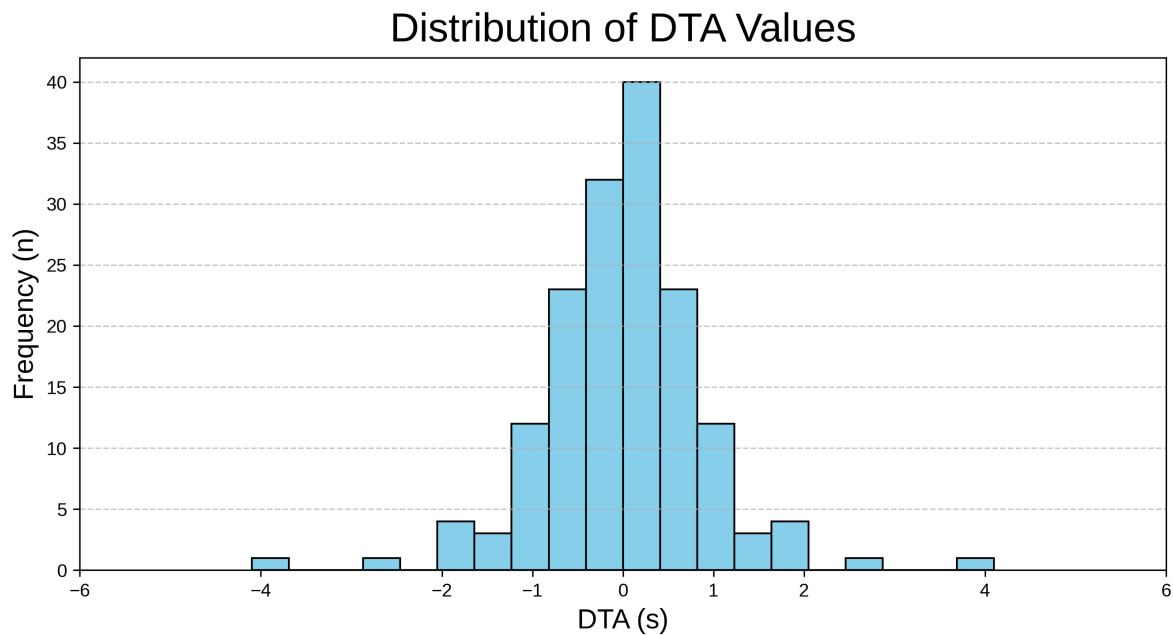
G.3. DTA distribution

Figure G.3: The distribution of DTA values for each participant across all trials. The histogram indicates that the highest occurrence of DTA values is within one second. Although the histogram may appear asymmetric, this is due to four instances where cyclist pairs exhibited a DTA of zero. The maximum DTA observed is approximately four seconds, corresponding to the detected passage described in the main text. This large DTA value resulted from a participant experiencing difficulty mounting the bicycle, which eliminated the need for significant path adjustments or modifications in selected velocity. An average DTA of 0.6 seconds was found.